Ibuprofen loading into Mesoporous Silica Nanoparticles using Co- Spray Drying : a Multi-Scale Study

Lucas Ruffel, Jeremy Soulié, Yannick Coppel, Pierre Roblin, Fabien Brouillet, Christine Frances, Mallorie Tourbin

The content of this manuscript is published in the article in press under the reference:

L. Ruffel, J. Soulié, Y. Coppel, P. Roblin, F. Brouillet, C. Frances, M. Tourbin, Ibuprofen loading into Mesoporous Silica Nanoparticles using Co-Spray Drying : a Multi-Scale Study, Microporous and Mesoporous Materials,
https://doi.org/10.1016/j.micromeso.2019.109689

Ibuprofen loading into Mesoporous Silica Nanoparticles using Co-Spray Drying : a Multi-Scale Study

Lucas Ruffel[1], Jérémy Soulié[2*], Yannick Coppel[3], Pierre Roblin[1], Fabien Brouillet[4], Christine Frances[1], Mallorie Tourbin[1*]

[1] Laboratoire de Génie Chimique, Université de Toulouse, CNRS, INPT, UPS, Toulouse, France.

[2] CIRIMAT, Université de Toulouse, CNRS, INP- ENSIACET, 4 allée Emile Monso, Toulouse, France.

[3] Laboratoire de Chimie de Coordination, CNRS UPR8241, Université de Toulouse, Toulouse, France.

[4] CIRIMAT, Université de Toulouse, CNRS, Université Toulouse 3 – Paul Sabatier, 35 Chemin des Maraîchers, Toulouse, France.

*corresponding authors : jeremy.soulie@ensiacet.fr, mallorie.tourbin@ensiacet.fr

ABSTRACT

Mesoporous Silica Nanoparticles (MSN) are used in an increasing number of applications in nanomedicine. Their synthesis and external/internal functionalization have been extensively studied as well as their biological properties. Nevertheless, the conventional drug loading processes of MSN (such as impregnation), do not enable sufficient efficiency and are difficult to consider on an industrial scale. To overcome these limitations, we implemented an innovative co-spray-drying process, using a nano spray-dryer, to load MSN with ibuprofen molecules. In this contribution, complementary techniques were used to perform a multi-scale characterization of the loaded particles. Spray-dried powders have been analysed from aggregates size and morphology to pore loading and ibuprofen conformation. This study demonstrates that ibuprofen/silica weight ratio in the initial suspension strongly affects the location (into

mesopores or external) and the conformation (crystallized, amorphous or liquid-like) of ibuprofen. The quantification of each phase has allowed calculating precise loading rates and demonstrate tunable pore filling.

KEYWORDS : Mesoporous silica nanoparticles, drug loading, spray-drying.

1. INTRODUCTION

During the last decade, Mesoporous Silica Nanoparticles (MSN) have been increasingly studied for various therapeutic and diagnostic applications, and in particular for cancer treatments [1,2,3,4].As other nanosystems like liposomes or dendrimers, MSN act as nanocarriers, delivering therapeutic (bio)molecules to a targeted location (cancer cell, tumor), preventing or restricting severe side effects. MSN are of huge interest because their numerous and complementary ways of elaboration allow finely tuning their properties. Among them, four properties strongly impact their efficiency[3,5] :

- Nanoparticles size and morphology/aspect ratio as they influence localization and internalization of MSN in the body [1,6],
- Pore diameter, morphology (hollow sphere, interconnection) and organization (hexagonal, radial, worm-like) that are predominant for drug loading and release (diffusion, dissolution) [7,8],
- External and internal functionalization [9] The external (bio)functionalization could have two main purposes: (a) Selective targeting for localized therapy using functions able to selectively interact with specific overexpressed receptors, (b) smart control of drug delivery thanks to gatekeepers that are (bio)organic stimuli-responsive entities blocking or opening pores [3,10,11]. The internal functionalization enables a better interaction between the drug molecules and the nanocarriers and could have an influence on the drug release[12,13,14],
- MSN loading processes / mechanisms (especially with hydrophobic drugs) and consequently the optimization of loading rate considering the available specific surface area and/or pore volume.

While the three first properties have been extensively described in the literature, the last one have been much less studied. Several processes may be used for drug loading. The easiest technique is commonly called impregnation. It consists of putting in extended contact MSN and a saturated drug solution. The solvent (usually organic) is then removed by evaporation (heating), centrifugation or filtration but the powder recovery yield is not optimized [15]. This method is driven by the thermodynamic equilibrium between solvated ibuprofen molecules and those physisorbed into mesoporous silica and the associated diffusion[16,17] Melt quenching is based on the mix of MSN and drug when heated in order to melt the latter, which helps the active substance to be loaded in the material; then, a quench is realized with liquid nitrogen. The main limiting parameter is the loading efficiency and its localization due to the viscosity of the molten drug [18]. A third alternative is the manual mixing where two different solids (silica matrix and drug) are put in a mortar and mixed manually with a pestle [19] However, these different techniques (manual mixing, melt quenching) are hard to optimize [15,19] and result in poor loading rates. Moreover these processes cannot be easily transferred on an industrial scale. Complete studies, considering several parameters (mesoporous structure, functionalization)[20] and including fine characterizations (NMR, SAXS, TEM) [19,21,22,23,24,26] have been carried out on mesoporous silica loaded thanks to previous processes. These articles were mostly focused on mesoporous silica under powder form composed of micron-scale grains with larger diffusion pathway for molecules into the mesoporous network, comparing to nanoparticles.

Compared to the above mentioned drug loading processes, the co-spray drying process seems to have a high potential. Currently used in the industry to produce a dry powder from a solution or a suspension, the spray-drying allows to load an active substance in a matrix, with a final product in a stabilized form [27,28] It has some benefits like the process duration and the recovery yield of the powder [19]. The greatest advantage of the spray-drier is its ability, in one step, to load the drug and separate the loaded product from the solvent by drying it. Nano spray-dryers allow highly efficient nanoparticles recovery thanks to electrostatic collection system [29,30,31,32]. One article [19] has been published on the use of a mini spray dryer to load micronic mesoporous

silica, but to the best of our knowledge, there is no description related to mesoporous silica nanoparticles combined with the use of a nano spray-dryer and especially with full and multi-tool characterization.

In this context, the aim of the present work consists in developing the co-spray-drying process with nano spray-dryer for the effective loading of a model molecule into MSN. Ibuprofen has been chosen due to its physico-chemical properties (slightly water-soluble) and its molecular size. Moreover, a good knowledge of its properties is made possible thanks to an abundant literature [33,34,35,36] The impact of MSN/ibuprofen ratio in the initial suspension (before spray-drying) on morphological and structural properties of resulting powders will be especially studied thanks to complementary techniques such as MEB, SAXS, solid state NMR, N_2 adsorption, MET. Consequently, this paper aspires to: i) highlight the mechanisms leading to the multi-scale organization of MSN loaded with ibuprofen (from micronic agglomerates size to the molecular conformation), ii) determine the correlation between the different ibuprofen states and their location (internal/external) and quantify the proportion of each state to calculate precise pore loading rates.

2. EXPERIMENTAL

2.1 Materials: Tetraethyl orthosilicate solution (TEOS, ≥99%), Hexadecyltrimethylammonium bromide powder (CTAB, ≥98%) and sodium hydroxide pellets (NaOH, ≥98%) were purchased from Sigma Aldrich. Ibuprofen 50 powder was purchased from BASF (particle size around 50 µm). Technical ethanol (96%), used for filtrations, was purchased from Acros Organics and absolute ethanol (≥99.8%), used for loading experiments, was purchased from Fisher Chemical. Deionized water (18.2 $M\Omega.cm^{-1}$) was used for the particle synthesis and the filtrations.

2.2 Nanoparticle synthesis: Mesoporous Silica Nanoparticles (MSN) have been synthesized by the sol-gel technique in a basic media, with TEOS as silica precursor and CTAB as cationic surfactant [16,37,38]. Briefly, 1.0 g of CTAB and 7 mL of NaOH (2 $mol.L^{-1}$), were added in 960 mL of deionized water inside a double-jacketed reactor (1 L, four waffles) at 80 °C. The solution was

mixed by mechanical stirring at 175 rpm for 30 min with an A310 axial flow impeller (Lightin). The stirring rate was next increased to 550 rpm and 10 mL of TEOS were added in the reactor with a peristaltic pump (Masterflex L/S) at 120 $mL.h^{-1}$. After 2 hours, the solution was filtered (Sartorius 391 filter, particle retention=2-3 µmm) with a Büchner and the resulting filter cake was washed with 3x500 mL of deionized water and 3x100 mL of technical ethanol 96%. After freezing (12 h, -20 °C) and lyophilisation (24 h, -55 °C, 1 mbar) with a Alpha 1-2 LyoDisplay freeze-dryer (Christ), the resulting powder has been calcined overnight in a tubular furnace at 600 °C under air flow in order to remove CTAB. Several batches of MSN were synthesized in the same conditions. The resulting powders were controlled thanks to DLS, SAXS and N_2 adsorption. Then they were mixed in order to have a sufficient amount of powder with uniform properties to be used during the spray-drying experiments.

2.3 Drug loading by co-spray-drying: The co-spray-drying process was used to load the ibuprofen into silica mesopores with the Nano Spray-Dryer B-90 from Büchi Labortechnik AG. The Figure 1 illustrates the flowsheet of this apparatus [39].

Several experiments were performed varying the Ibuprofen/Silica mass ratio in the stock suspension (Figure 1-①) in order to analyse the effect of this key parameter on the MSN loading. The silica concentration stayed constant (5 $g.L^{-1}$). The volume of ethanol was calculated depending on the amount of silica, whereas the ibuprofen concentration was the variable parameter (from 1 to 20 $g.L^{-1}$, see Table 1 and Figure 2-a,b,c). This initial suspension was sonicated before the co-spray drying experiment during 5 min at 350 W (FB705 Fisherbrand Ultrasonic Processor), and stirred during all the process in order to facilitate the dissolution of ibuprofen and the dispersion of MSN. After the pumping of the suspension, droplets are generated with a piezoelectrically driven vibrating mesh (Figure 1-③); these droplets are formed with a narrow size distribution controlled by the membrane vibration (spray mesh size of 7 µm) [31,32]. A flow of hot nitrogen gas (70 °C, 35 mbar, around 95 $L.min^{-1}$) dries the droplets inside the drying chamber while evaporating the solvent (Figure 1-② and ④) and generates dried powder composed of particles

agglomerates. Then, the powder is collected with an electrostatic collector (Figure 1-⑤) instead of a cyclone technology as in conventional spray-dryers. A stainless steel cylinder allows to collect the particles because of a high voltage application between this electrode and a star-shaped counter electrode (cathode); spray dried powder is then charged and electrostatically deposited on the inner wall of the cylinder electrode. This mechanism is independent of particle mass (unlike for the cyclone technology) and is based on particles electrostatic charging.

The short configuration (height: 110 cm) of the drying chamber has been used. Due to the use of a fully organic solvent (ethanol), the spray dryer was combined with different Büchi accessories allowing to inert the system (Inert Loop B-295), avoid the presence of water (Dehumidifier B-296) and recycle the drying gas used with the Büchi Aspirator. ~~A sonication of the initial suspension was made before the co-spray drying experiment during 5 min at 350 W (FB705 Fisherbrand Ultrasonic Processor), facilitating the dissolution of ibuprofen and the dispersion of MSN.~~ After the spray drying, the powder was removed from the cylinder electrode through a particle scrapper.

2.4 Characterization: An important part of this work has been focused on the characterization of powders generated by spray-drying in order to have a better understanding of the influence of the mass ratio of ibuprofen over silica (noted R=ibu:Si thereafter) on the properties of the particles.

Dynamic Light Scattering (DLS): Hydrodynamic diameters of the MSN in suspension were obtained with a ZetaSizer Nano-ZS (Malvern Instruments Ltd). This equipment uses a laser (He-Ne at λ=633 nm, under voltage of 3 mV) and the detector is located at 173 ° to analyse the scattered intensity fluctuations. 10 mg of MSN were dispersed inside 20 mL of water with the ultrasonic processor [40] (5 min, 350 W) prior to the measurement performed at a temperature of 25 °C.

N_2 Adsorption: Nitrogen adsorption/desorption isotherms were performed to characterize the textural properties of the MSN and the spray-dried samples with a Tristar II (Micromeritics). The samples were vacuum outgassed at ambient temperature for 24 hours to remove physically adsorbed water molecules from the pores. Pore size distributions of the MSN were determined

from the desorption isotherm with the Barret-Joyner-Hallenda (BJH) method [41] The specific surface areas and pore volumes were determined from the linear portion of the Brunauer-Emmet-Teller (BET) plots [42].

Small Angle X-Rays Scattering (SAXS): The SAXS analyses were performed on XEUSS 2.0 (Xenocs Company) composed of X-ray microsource delivering at 8 keV a spot sized beam equal to 0.5 mm with an intensity close to $30*10^6$ photons.s^{-1}. The samples were placed on sample loader dedicated to powders with 387.5 mm of distance from the detector, providing a range of scattering vector starting from 0.02 $Å^{-1}$ to 1.6 $Å^{-1}$. The samples were exposed during 300 s under vacuum and the scattered beam was collected on the 1M Pilatus detector (1 million counts/pixel). Data integration and reduction were performed with the software FOXTROT.

Transmission Electron Microscopy (TEM): TEM images were taken by a JEM-1400 electron microscope (JEOL). The conditions were as follows: W filament, voltage of 120 kV, 3.8 Å of resolution. Scanning Transmission Electron Microscopy (STEM) tests were performed using a JEOL cold-FEG JEM-ARM200F operated at 200 kV equipped with a probe Cs corrector reaching a spatial resolution of 0.078 nm. The detector used is the High-Angle Annular Dark Field (HAADF).

Scanning Electron Microscopy (SEM): SEM has been used to study the morphology of agglomerated particles. Electron micrographs were taken using the secondary electron mode using a FEI 450 Scanning Electron Microscope (Quanta SEM), with a voltage of 12.5 kV.

X-Ray Diffraction (XRD): Powder X-Ray Diffraction was performed using a Symphonix 1000 (INEL). The X-ray source was a Co radiation (λ=1.7889 Å) and measurement conditions were as follows: voltage of 30 kV, current of 30 mA, room temperature, step size of 0.01 °. Samples were manually ground before measurements to randomize the orientation.

Thermogravimetric Analysis/Differential Thermal Analysis (TGA/DTA): TGA/DTA measurements were performed on a TGA-DTA SETSYS Evolution (SETARAM Instrumentation) under air flow. The samples were stabilized to 25 °C, then heated to 800 °C with a heating rate of 5 °C/min. The acquisition system used was SETSYS Ev 1750. TGA has not been carried out for 80:20 sample due to the lack of spray-dried collected powder.

Solid-state Nuclear Magnetic Resonance (NMR): Solid-state NMR experiments were recorded on an Avance III HD 400 spectrometer (Bruker). Samples were packed into 4 mm zirconia rotors which were spun at 8 to 10 kHz at 298 K. ^{1}H, ^{13}C and ^{29}Si MAS single pulse experiments were performed with recycle delays of 3 s, 5 s and 60 s, respectively. ^{13}C-CP/MAS and ^{29}Si-CP/MAS spectra were recorded with a recycle delay of 2 s and contact times of 2 ms and 3 ms respectively. ^{13}C MAS with Insensitive Nuclei Enhanced by Polarization Transfer (INEPT) were recorded with a recycle delay of 3s and interpulses delays synchronized with the spinning rate. A mixing time of 4 ms was used for ^{1}H-^{1}H NOESY experiment. All of the chemical shifts are relative to Tetramethylsilane.

3. RESULTS AND DISCUSSION

3.1 As-synthesized silica nanoparticles

As-synthesized mesoporous silica nanoparticles (MSN) have been analysed by means of several techniques. N_2 adsorption/desorption isotherm (Appendix A Figure S1) is type IV according to IUPAC[43] and nanoparticles exhibit a high BET [42] specific surface area of 806 $m^2.g^{-1}$. Pore size distribution has been calculated with the BJH theory [41] and pores diameter is centered around 2.9 nm (Table 2). These values are similar to those obtained in the literature for this type of system [19,22]. SAXS measurements (Figure 3-b) demonstrate a 2D hexagonal cylindrical network organization (P6mm) in honeycomb with the indexation of d_{100}, d_{110} and d_{200} peaks (respectively q_1, q_2 and q_3) and allows calculating the centre-to-centre distance, which is about 4.1 nm, in agreement with the literature [44] TEM pictures confirm the MCM-41 derived 2D hexagonal organization of pores (Figure 4) and highlight the spherical shape of particles. Their diameter varies from 100 to 250 nm (Appendix, A Figure S2-a). DLS completes this information by giving a hydrodynamic particle diameter distribution (Appendix A, Figure S2-b) of MSN suspension. Even if the diameter is overestimated (hydration layer) comparing to TEM, the distribution is monodisperse and quite narrow (PDI<0.3) with a modal diameter of 301 nm. Although the diameter of these particles seems to be high considering biomedical applications, they have been

chosen for their well-organized porosity. Indeed, smaller nanoparticles lead to disorganized or worm-like porosity for SBA or MCM-derived silica [45]. Considering that the aim of this article is the proof of concept of a possible efficient loading, well-defined porous network should be particularly adapted to characterize the state and organization of molecules into nanoparticles.

3.2 Morphology and composition of resulting agglomerates

After having performed the co-spray drying process with different ibuprofen/silica ratios in the stock suspension, complementary techniques were used to characterize the hierarchical organization of resulting dried agglomerates. For the Ibu:Si ratio 100:0 (w/w) (*i.e.* pure ibuprofen spray-dried), the quantity used is much higher than other ratios because the yield drastically dropped, due to the sticky behaviour of the product (Table 1).

SEM gives information about the spatial localization of silica particles and remaining solid ibuprofen (if any) into agglomerates. Figure 5 shows high magnification of powder grains for different ibuprofen/silica ratios (R). For spray-dried pure silica (R=0:100), MSN are spherically agglomerated and organized with a hollow sphere shape (Figure 5-a). This morphology is typical of fast solvent evaporation (ethanol) in the drying chamber (Figure 1-④) during the spray-drying process [46,47,48,49]. When ibuprofen is added in the initial suspension and the ibuprofen quantity is increased, the previous morphology is preserved for the dried agglomerates formed at R=25:75 (Figure 5-b) and 50:50 (Figure 5-c), even so the central hole is less well-defined. Considering low magnification pictures (Appendix A Figure S3), the diameters of agglomerates are between 1 and 7 µm with a broad size distribution for these three conditions. These results imply that, for these ratios, ibuprofen molecules are either entrapped inside mesopores or present as small nanometric entities (undetectable with conventional SEM) between silica nanoparticles. For higher ratio (R=80:20), agglomerates have irregular shapes (Figure 5-d) with higher particle sizes between 10 and 40 µm. Interestingly they are mainly composed by a continuous matrix on which silica particles are agglomerated. Due to the high amount of ibuprofen compared to silica

for this sample, we can assume that this matrix is ibuprofen in a solid state. Globally, SEM pictures suggest that the ibuprofen could get different locations depending on the Ibu:Si ratio.

For pure ibuprofen, the resulting grains are bigger with sizes of several hundred microns with an important roughness (Figure 5-e). These final grains may have a flat shape due to the surface of the electrode (flattening of the grain due to the attractive force the electrode).

This could be enhanced by remaining ethanol in ibuprofen during the collection, which make the powder stickier and more deformable. This phenomenon may have been avoided for samples containing silica particles, the later increasing the mechanical properties (stiffness) of the resulting composite. Beyond location of ibuprofen, some selected X-ray diffraction patterns are presented on Figure 6 (totality of patterns on Appendix A Figure S4) to check its physical state when dried. For free-ibuprofen sample (R=0:100), a very broad halo centred around 26 ° is observed. It is characteristic of the short-range order (SiO_4 tetrahedra) of amorphous silica. This broad halo is still present when the ibuprofen amount is increased regardless the sample, except for the 80:20 ratio. Nevertheless, a series of additional sharp peaks are present from the 40:60 to the 100:0 ratios. These sharp peaks become more and more intense as the ibuprofen percentage increases in the stock suspension. These diffraction peaks were attributed to crystalline ibuprofen (main peaks with following values of 2θ: 14.1, 19.3, 23.4, 25.9 and 32.2°) [19]. It corresponds to the most thermodynamically stable phase (α) with a P21/c symmetry. These results demonstrate that below the 40:60 ratio, ibuprofen does not form crystal. It could be correlated with the previous hypothesis assuming that the molecules are located into mesopores for these ratios. It has been proved that the crystallization of a molecule can occur in channels only if the channel diameter/molecular size ratio is more than 20.[50] In our case, the pore diameter is about 3 nm (Table 2, Figure 7) and the ibuprofen molecule is about 11.5 Å long [22]. Thus, the size of mesopores avoids the formation of ibuprofen crystals inside them. Combining SEM pictures and XRD, we can assume that beyond the 40:60 ratio, nanocrystals of ibuprofen are formed out of porosity and tends to agglomerate. The hypothesis of the nanoscale of crystals is supported by the

width of ibuprofen peaks resulting of small crystalline domains (Appendix A Figure S5). The crystallite size has been calculated for pure spray-dried ibuprofen thanks to the Scherrer equation applied to the [200] peak and is around 40 nm. The presence of ibuprofen nanocrystals is consistent with the spray-drying process. Indeed, the ethanol solvent evaporation is very fast, promoting nucleation over growth. This trend may have been accentuated for samples containing silica as each particle could enhance heterogeneous nucleation.

Thermogravimetric Analysis (TGA) has been used to quantify the ibuprofen amount. TGA curves are presented in Figure 8-a. For pure spray-dried ibuprofen (R=100:0) and considering the derivative of its curve, two main mass losses occur: the first one between 136 and 280 °C and the other one between 280 and 345 °C. Three main peaks could be observed on corresponding TGA results (Figure 8-b): two endothermic peaks, respectively at 80 and 259 °C and an exothermic peak at 288 °C. According to the literature [51] these peaks can be respectively attributed to the melting point, the boiling point and the degradation (oxidation) of ibuprofen, meaning that the first mass loss is due to ibuprofen evaporation and the second one to its decomposition. With the same methodology, three zones have been determined for pure silica nanoparticles. Below 150 °C, the first zone corresponds to the desorption of physisorbed water or ethanol (endothermic peak centred around 68 °C). Between 150 °C and 236 °C, a plateau is observed and above 236 °C, the weight loss is attributable to de-hydroxylation, *i.e.* the surface silanols condensation [52] For samples containing both ibuprofen and silica, two domains separated by a clear break can be distinguished. This break occurs at 355, 344, 370 and 366 °C for respectively 20:80, 25:75, 40:60 and 50:50 samples and is correlated to intense exothermic peaks suggesting that they could be linked to ibuprofen degradation. It is interesting to note that endothermic peaks related to melting point of crystalline ibuprofen is only present for samples with initial Ibu:Si ratios above 40:60 (Figure 8-b). These results can be correlated with those of XRD. Indeed, the melting temperature is only observed when crystals are detected. In any case, several points can be assumed: i) Below 150 °C the mass loss is only due to the removal of physisorbed remaining water or ethanol. ii)

Above this value the mass loss is related to ibuprofen removal (evaporation and/or degradation). iii) At 800 °C the resulting material is de-hydroxylated silica. iv) The amount of silanol groups at the surface of silica is the same whatever the samples. Indeed, all particles are taken from the same lot (combination of different synthesis batches) and the conditions in the initial suspension and during the spray-drying process are not severe enough to remove them (deprotonation, internal condensation) as demonstrated below by NMR. Considering these hypothesis, it is possible to calculate the weight percentage of each entity and especially of ibuprofen. Results are presented in Table 3. Residual water/ethanol amount in the dried samples decreases when ibuprofen increases. It seems consistent, as the number of ibuprofen molecules interacting with the silica matrix is increased (assuming that part of ibuprofen is inside the pores). Consequently, it reduces the probability of silanol interactions with small physisorbed molecules. Moreover, the ibu:silica weight ratio in spray-dried powders reaches lower values comparing to those in the stock suspensions. This difference may be explained by the potential loss of isolated nano-agglomerates of ibuprofen molecules carried away by the gas flow.

3.3 Pore filling and ibuprofen conformation

The honeycomb network of the MSN seems to be unmodified by the presence of ibuprofen (TEM analysis, Appendix A Figure S6). Although TEM pictures allow directly observing the porous network, they do not reveal any changes between initial MSN and silica particles co-spray-dried with ibuprofen. The difficulty in observing it could be explained by the combination of two factors: i) as ibuprofen is mainly constituted by carbon, the difference in electronic density between ibuprofen-filled pores and silica network should not exhibit high contrast, ii) at the particle scale, the superposition of porous channels makes it difficult to distinguish the pore filling.

On the contrary, SAXS reveals important changes when ibuprofen and silica are co-spray-dried. SAXS curves for MSN, for pure spray-dried silica and for samples with different ratios are presented on Figure 3-a. Until 0.1 $Å^{-1}$, the domain (I) reveals that the negative slop of curves is increased with the increase of ibuprofen ratio. MSN and R=0:100 (spray dried MSN) samples

curves have slope close to q^{-3} whereas that of 80:20 is close to q^{-4}. As these slopes are related to the surface state in the Porod domain, it could mean that the roughness of silica spheres is step by step reduced. It is consistent with SEM and XRD analyses. Indeed, between 30:60 and 40:60 ratios, a layer of agglomerated ibuprofen nanocrystals is progressively formed at the surface of nanoparticles after this molecule has filled pores. It could explain the "smoothing" of particles surface due to the homogeneity of this ibuprofen layer with low spatial variations of electronic density. The domain (II) (approximatively from 0.1 $Å^{-1}$ to 0.4 $Å^{-1}$) is the one that is most usually studied in the field of structured mesoporous materials, as these peaks are due to the diffraction of x-rays by the empty pores mesostructure due to high contrast of electronic density with silica matrix. First, these curves confirm that the silica structure is not modified during the co-spray-drying with or without ibuprofen. As q_1, q_2 and q_3 peaks have the same value for all the samples and the q_2/q_1 and q_3/q_1 values are close to each other (Table 4), we can guess that the P6mm structure remains the same with similar distance from centre to centre of adjacent cylindrical pores (about 4.1 nm). However, the peak intensity decreases as the ibuprofen amount increases. This phenomenon could be explained by the decrease of the electronic density contrast between silica and ibuprofen (mainly composed of carbon) filling the pores. Thus an intensity decrease indicates the gradual filling of pores. This kind of contrast decrease has already been described for micron-scale SBA-15 or MCM-41 particles filled by ibuprofen [20,53,54] or naproxen [26] and characterized by SAXS or SAXRD. On the contrary, the increase of contrast is associated to the presence in pores of entities with higher electronic densities like iron oxide [55] or metallic copper [56]. Finally, domain (III) crosschecks the information obtained by XRD on the structural organisation of ibuprofen molecules. The filling is still improved for 50:50 and 80:20 ratios, meaning that the crystallisation of ibuprofen outside of particles revealed by XRD does not occur because of a lack of free pore surface/volume for molecules.

To complete the understanding of pore filling, N_2 adsorption measurements have been carried out (Table 2). BET calculations reveal two tendencies of the specific surface area with an increase in

the amount ibuprofen: i) first, it drastically and continuously decreases from 0:100 (787 $m^2.g^{-1}$) to 35:65 (23 $m^2.g^{-1}$). Within the same ratio domain, the pore volume goes from 0.657 $cm^3.g^{-1}$ when there is no active substance (R=0:100) to 0.045 $cm^3.g^{-1}$, meaning that the specific area diminution is related to mesopores filling. ii) Secondly, the specific surface area remains the same for 35:65, 40:60 and 50:50 samples (around 25 $m^2.g^{-1}$) as well as the pore volume (around 0.045 $cm^3.g^{-1}$). In order to explain these results, two consecutive stages of pore filling need to be considered. The first one is due to ibuprofen physisorption during the first step, in the initial suspension. As there is a thermodynamical equilibrium, the suspensions (regardless the concentration) are composed of adsorbed and free molecules, and could be described as a Langmuir-type isotherm [17,57]. Results on the 100:0 sample demonstrate that free molecules crystallize during the spray-drying process and the solvent evaporation. No crystalline phase is observed until 40:60 ratio (see XRD on Figure 6). It could be explained by the second step of loading: the solvent evaporation during the drying process leads to a diffusion of the molecules from the solvent of the droplets to the pores [58], modifying the previous organization of ibuprofen. Pore size distribution has been calculated thanks to the BJH model (Figure 7). Modal pore size diameters (Table 2) slightly decreases when increasing the amount of ibuprofen from 2.9 nm for pure spray-dried silica to approximatively 2 nm for samples for which no crystallisation is observed (until R=35:65). No modal diameter can be given beyond this ratio, because no clear maximum appears in the mesoporous range. These results need to be carefully considered as this is the limit of the BJH theory [41], but we can reasonably suppose that the loading is first due to the formation of a layer inside mesopores for samples with low initial ibuprofen concentration. For higher ibuprofen amount (from R=40:60), the N_2 molecules can no longer fill the pores (reduction of the specific surface area) because of an increase of volume loading of ibuprofen (vs. previous surface loading). This low specific surface is also induced by the crystalline ibuprofen matrix around the MSN composed by previously free ibuprofen molecules that have not diffused into the pores during the evaporation of ethanol. Similar results have been obtained and explained by probing occluded void space inside MCM-41 channels with ^{129}Xe NMR.[59] Considering this hypothesis, the

improvement of filled pores percentage observed by SAXS (decrease of the q_1 peak intensity between R=50:50 and R=80:20) for higher ratios could also be explained even so the specific area remains the same. Indeed, as the ratio of ibuprofen was higher in the initial suspension, and considering the equilibrium between free molecules and adsorbed molecules, the amount of physisorbed molecules should be higher. It could lead to an increased filling rate (Figure 2-d,e,f).

Various NMR experiments have been achieved to gain information on ibuprofen behaviour at the molecular scale. No clear difference for samples from 20:80 to 100:0 could be observed by ^{29}Si MAS and CP/MAS NMR experiments (Appendix A Figure 7). This confirms that the structure of mesoporous silica is not modified by the ibuprofen addition. Notably the ^{29}Si CP/MAS experiments, that enhance the Q^2 ($Si(OSi)_2(OH)_2$) and the Q^3 ($Si(OSi)_3(OH)$) silicon signals evidence that there is no detectable dehydroxylation of the silica.

Carbon atoms have been probed using ^{13}C MAS and CP/MAS NMR experiments for several samples from 0:100 to 100:0 and for commercial crystalline ibuprofen and a solution of ibuprofen in ethanol (Figure 9 and Figure 10). As expected, for ibuprofen in solution very sharp peaks are observed in ^{13}C MAS experiment while no signal is detected in the ^{13}C CP/MAS experiment (^1H-^{13}C dipolar coupling average to zero due to the fast tumbling motion in solution). On the contrary, for the well-crystallized commercial phase, ^{13}C signal is easily seen with the CP/MAS experiment while the detection is more difficult with ^{13}C MAS experiment due to the very long ^{13}C T_1 relaxation times (e.g. $T_1 > 50$ s for aromatic and carbonyl carbons) (Figure 9). With a relaxation delay of 5 s, the signal of mobile alkane groups that possess shorter T_1 are much more intense than the ones of aromatic and carbonyl groups. ^{13}C MAS spectra of spray-dried ibuprofen (100:0 sample) are very similar to the ones of the commercial crystalline sample. However, the ^{13}C signals are slightly broader (especially for the aromatic carbons 5-8, see Appendix A Figure S8) and the relative intensities of the aromatic signals in the ^{13}C MAS experiment are slightly higher (shorter T_1 than in the crystalline powder). This indicates that the spray-dried ibuprofen is less crystallized than the commercial one. The ^{13}C MAS spectra of samples 20:80, 25:75, 35:65 are very similar to the

dissolved ibuprofen one. This kind of result has been previously described and it is characteristic of ibuprofen adopting a liquid-like behavior inside the silica mesopores [22]. The most important change is a shift of the carbonyl signal from 177.4 ppm for ibuprofen in ethanol solution to 179.4 ppm for the 20:80 to 35:65 samples. This shift is probably related to a change in the hydrogen bond network of the carbonyl group (dimer formation, interaction with ethanol OH groups,..). However contrary to the ethanol solution, few weak ^{13}C CP/MAS signals for the most rigid parts of the ibuprofen molecules could be detected for the 20:80 to 35:65 samples evidencing some mobility restriction of ibuprofen in the pores. This hypothesis is reasonable, as the molecule is approximatively 11.5 Å long in a 2.9 nm diameter pore and ibuprofen mobility can be reduced due to steric hindrance. For the 40:60 sample, ^{13}C CP/MAS shows a new set of intense ibuprofen resonances that correspond to crystallized ibuprofen molecules.

This result is reliable with XRD for which the crystalline phase is first detected for the 40:60 sample. These crystalline phase signals have weak intensities in the ^{13}C MAS spectrum. The methyl 3 ^{13}C MAS signal can be used to measure the different phase population: i) it shows different chemical shift for the solid and liquid-like phase at 14.7 and 17.5 ppm, respectively (Appendix A Figure S9); ii) the ^{13}C T_1 of this group is similar in both phases with a short value of 1.0 s. For the 40:60 sample, the crystallized ibuprofen phase represents 7±2 % of the total ibuprofen. For the 50:50 and 80:20 samples, a strong increase of the relative proportion of the solid ibuprofen phase is observed in the ^{13}C CP/MAS and MAS experiments. Moreover, the shapes of the carbonyl and aromatic carbon resonances are complex and result from the superposition of sharp resonances (crystallized form) and broad ones (amorphous form). The relative proportion of the amorphous phase increases for the 80:20 sample compared to the 50:50 one with crystallized/amorphous ratios of 40/60 and 55/45, respectively (determined by signal deconvolution). ^{13}C MAS experiments also evidence a broadening of the liquid-like phase resonances for the 40:60 to 80:20 sample. It could be the sign of a partial structuration of ibuprofen molecules confined into the mesopores when the ibuprofen amount is increased. This hypothesis is confirmed by the ^{13}C

INEPT MAS experiments (Appendix A Figure S10) that allow detection of very mobile ibuprofen molecules. The ^{13}C INEPT signal intensities are strong for 20:80 and 25:75 samples. These signals then decrease continuously from 35:65 to 80:20 samples indicating a notable diminution of the mobility of ibuprofen into the mesopores with an increase of ibuprofen amount inside them. It is consistent with the previous hypothesis (from SAXS and N_2 adsorption results, see Figure 2-d,e,f), in which the amorphous phase results of ibuprofen densification inside the pores. This amorphous phase is the most dense phase that can be found in the pores, because these don't reach the required size to allow ibuprofen crystals formation. As the ibuprofen concentration is increased in the stock suspension, both solvated and physisorbed ibuprofen amounts are increased due to the thermodynamic equilibrium. However, this "amorphous condensed phase" has never been observed for MSN loaded by impregnation. It means that the evaporation process should play a key role in the densification of ibuprofen into the pores. Then, for ratios higher than 40:60, the chronological steps of ibuprofen evolution could be the following (Figure 2): i) stock solution with free and physisorbed (liquid-like) ibuprofen, ii) spray-drying process increasing the amount of "internal ibuprofen" by densification (solid amorphous phase) due to the diffusion of previously "free" ibuprofen into the pores induced by the ethanol evaporation, iii) crystallization of remaining free ibuprofen still during spray-drying. Consequently, for these samples , both internal (densification from liquid-like to amorphous) and "external" (crystallized) forms are enhanced. The deconvolution of corresponding solid state NMR peaks allows determining the proportion of liquid-like, amorphous and crystalline ibuprofen. By combining these results (Table 5) with TGA results (silica/total ibuprofen ratio), it is possible to calculate the ratio (R_{exp}) between "internal" ibuprofen (liquid-like + amorphous) and silica. Assuming a total and dense loading of the porous network, the ibuprofen / silica ratio (R_{theo}) can also be approximated : the amount of ibuprofen is obtained by considering the pore volume of MSN Vp = 0.754 $cm^3.g^{-1}$ and the density of condensed crystalline ibuprofen i.e. d = 1.076 $g.cm^{-3}$ [25]. Finally, the pore loading rate is estimated by the comparison (R^{exp}/ R^{theo}) of these ratios (Table 5). It can be observed that the pore loading rate quickly increases from R=20:80 to R=40:60. This increase slows down after the

apparition of solid ibuprofen phases (amorphous and crystalline), with a pore loading rate barely to 60% for R=50:50. This good loading rate is close to those described in the literature [16] for impregnation (approximatively corresponding to 30 wt% of ibuprofen) but in this case with a continuous, robust and faster process. This loading rate could be improved (and the amount of crystallized/external ibuprofen decreased) by optimizing some of the parameters of the spray-drying process such as the drying temperature or the concentration of the initial suspension.

^{1}H MAS NMR gives additional information on the ibuprofen/silica system. Due to strong ^{1}H-^{1}H dipolar couplings, the ^{1}H signal of solid ibuprofen are very broad as usual (Figure 11). On contrary, the liquid-like phase shows sharp signals due to strong reduction of dipolar couplings associated with fast motions. As for ^{13}C MAS results, ^{1}H MAS NMR of samples 20:80 to 40:60 are very similar to the dissolved ibuprofen one. Continuous broadening of ^{1}H resonances with increase of ibuprofen amount is also observed especially for ratio above 35:65 (notably for hydrogen 10). It confirms the reduction of the mobility of ibuprofen located into the mesopores when the ibuprofen concentration increase. The spray-dried silica (100:0) shows mostly a broad signal at 4.9 ppm corresponding to hydrogens of SiOH groups in fast exchange with hydrogens of physisorbed water molecules. This signal continuously shift from 5.2 to 6.5 ppm for 20:80 to 50:50 samples. This shift is probably the result of several contributions: i) removing water molecules evidence by TGA analyses, ii) increase contribution of ibuprofen OH groups detected at 6.2 ppm in ethanol solution, iii) possible formation of hydrogen bonds between SiOH and ibuprofen carboxylic group and iv) ring current effect of the ibuprofen aromatic cycle. Anyway, this OH signal shift confirms the increase concentration of ibuprofen inside the mesopores. Note that the OH signal goes back to 6.4 ppm for 80:20 sample possibly due to a weak water contamination.

No information about ibuprofen/silica interaction could be obtained by ^{1}H/^{29}Si HETCOR experiments where only correlations between OH groups and silicon atoms are observed (not shown). ^{1}H NOESY experiment (notably performed for the 35:65 sample) on contrary, shows cross-peaks between OH hydrogens and different ibuprofen hydrogens associated to spatial proximities (SI Figure S11). As NOE cross-peaks of similar intensities are observed with methyl

groups on each side of the molecules (methyls 3, 12 and 13) but also with the aromatic hydrogens (5-8), it can be concluded that there is no preferential orientation of the ibuprofen molecules into the mesopores. In fact, only the less accessible alkane groups 10 and 11 do not show NOE cross-peaks with the OH hydrogens. This is in line with the important mobility of ibuprofen in the pores. Indeed, in the case where strong interaction between ibuprofen and silica may have been present (through hydrogen bond for example), the ibuprofen mobility should have been weaker and specific NOE correlations should have been observed.

4. CONCLUSION

An innovative nano-co-spray-drying process has been used for the first time to load mesoporous silica nanoparticles (diameter of 300 nm/pore size of 2.9 nm) with ibuprofen molecules. Multi-scale advanced characterization techniques provided key results on the location and the state of ibuprofen depending on the ibuprofen/silica ratio in the initial suspension:

- Micrometric agglomerates obtained by spray-drying go from spherical hollow spheres at low ibu:silica weight ratios, to irregular shapes and larger sizes at higher ratios.
- The drug loading of the MSN is the result of two consecutive stages of pore filling: ibuprofen physisorption in the initial suspension and then diffusion of the ibuprofen molecules into the pores driven by the solvent evaporation during the spray-drying process.
- Up to 35:65 ibu:silica weight ratio, ibuprofen is encapsulated into the mesopores and adopts a liquid-like behavior. The amount of encapsulated ibuprofen continuously increases with the initial ibuprofen concentration.
- At 40:60 ratio, a crystalline ibuprofen phase appears out of the porous network and its amount increases for higher ratios. A second “solid” phase is detected at the 50:50 ibu:silica ratio and could be explained by a densification of intraporous ibuprofen.

Beyond mechanistic and fundamental aspects, the identification and quantification of the state of loaded drugs and the fine calculation of loading rates are of major interest for the industrial

transfer of such a process. This work is the first step of the drug loading optimization that will require an exhaustive study of the effects of other spray-drying parameters.

ACKNOWLEDGMENTS

The authors would like to acknowledge Marianne Clerc-Imperor for helpful discussions about SAXS results, Gwénaëlle Guittier (LGC) for N_2 adsorption measurements and Cédric Charvillat (CIRIMAT) for XRD and TGA-TDA measurements. They also want to thank Alessandro Pugliara and Teresa Hungria (Centre de MicroCaractérisation Raimond Castaing UMS 3623) and Stéphanie Balor (METi) for the TEM analyses. The FERMaT Federation FR3089, Université de Toulouse, CNRS is acknowledged too for providing Small Angle X-Ray Scattering laboratory facility.

TABLES

Table 1: Spray-dried samples labelling depending on silica and ibuprofen mass in the initial suspension.

Samples (R=Ibu:Si)	**0:100**	**20:80**	**25:75**	**30:70**	**35:65**	**40:60**	**45:55**	**50:50**	**80:20**	**100:0**
m_{silica} (mg)	400	629	501	478	426	401	376	375	200	0
$m_{ibuprofen}$ (mg)	0	157	168	204	231	269	309	376	800	12010

Table 2: Surface properties obtained by nitrogen adsorption of MSN and spray-dried samples at different ibuprofen/silica weight ratios (R)

Sample (R=Ibu:Si)	**Specific area ($m^2.g^{-1}$)**	**Pore volume ($cm^3.g^{-1}$)**	**d_{BJH} (nm)**
Initial MSN	806	0.754	3.0
0:100	787	0.657	2.9
20:80	477	0.357	2.2
25:75	266	0.196	1.9
30:70	132	0.115	2.0
35:65	23	0.045	-
40:60	23	0.043	-
50:50	25	0.044	-
100:0	0.43	0.006	-

Table 3: Weight percentages of different entities in spray-dried powders (calculated thanks to TGA curves). Ibuprofen on silica weight ratios in the spray-dried powders and the initial suspensions. For spray-dried samples, ratios have been calculated considering that silica weight is the summation of de-hydroxylated silica and surface hydroxyl groups.

	Spray-dried powder				Ibu : silica weight ratio	
Sample	De-hydroxylated SiO_2 wt%	OH groups wt%	Physisorbed entities H_2O/EtOH wt%	Ibuprofen wt%	Spray-dried powder	Initial suspension
0:100	88.94	6.1	4.96	0.00	0.00	0.00
20:80	76.72	6.1	3.58	13.60	0.16	0.25
25:75	67.89	6.1	3.33	22.68	0.31	0.33
40:60	61.35	6.1	2.89	29.66	0.44	0.67
50:50	55.96	6.1	2.94	35.00	0.56	1.00

Table 4: Ratios of scattering vector values (SAXS) of diffraction peaks (q_2/q_1 and q_3/q_1) related to the mesoporous network and calculated centre-to-centre pores distances (a).

	Theoretical values for hexagonal organization (P6mm)	**MSN**	**0:100**	**20:80**	**25:75**	**30:70**	**35:65**	**40:60**	**45:55**	**50:50**	**75:25**	**100:0**
q_2/q_1	1.732	1.740	1.731	1.742	1.740	1.720	1.728	1.728	1.728	1.740	1.706	No silica
q_3/q_1	2.000	2.008	1.996	1.996	2.008	1.985	1.997	1.985	1.985	2.008	1.974	
a (nm)	-	4.115	4.187	4.180	4.220	4.204	4.237	4.245	4.245	4.220	4.270	

Table 5: Quantification of different ibuprofen states by NMR spectroscopy. The pore loading rate has been calculated combining NMR, TGA and N_2 adsorption results.

Theoretical ibu:Si (w/w) ratio		**20:80**	**25:75**	**40:60**	**50:50**
Ibu:Si (w/w) ratio calculated by TGA		14:86	23:77	30:70	35:65
Internal	**Liquid-like (%)[a]**	14	23	28	23
	Amorphous (%)[b]	n.d.	n.d.	n.d.	5
External	**Crystalline (%)[b]**			2	7
« Internal ibu »:Si molar ratio		4:96	8:92	10:90	11:89
Pore loading rate		21%	42%	53%	58%

n.d.: Not detected. [a] measured from area integration of methyl 3 resonance in ^{13}C MAS experiments. [b] determined from signal deconvolution of carbonyl 1 resonance in ^{13}C CP/MAS experiments both included in solid ibuprofen.

FIGURES

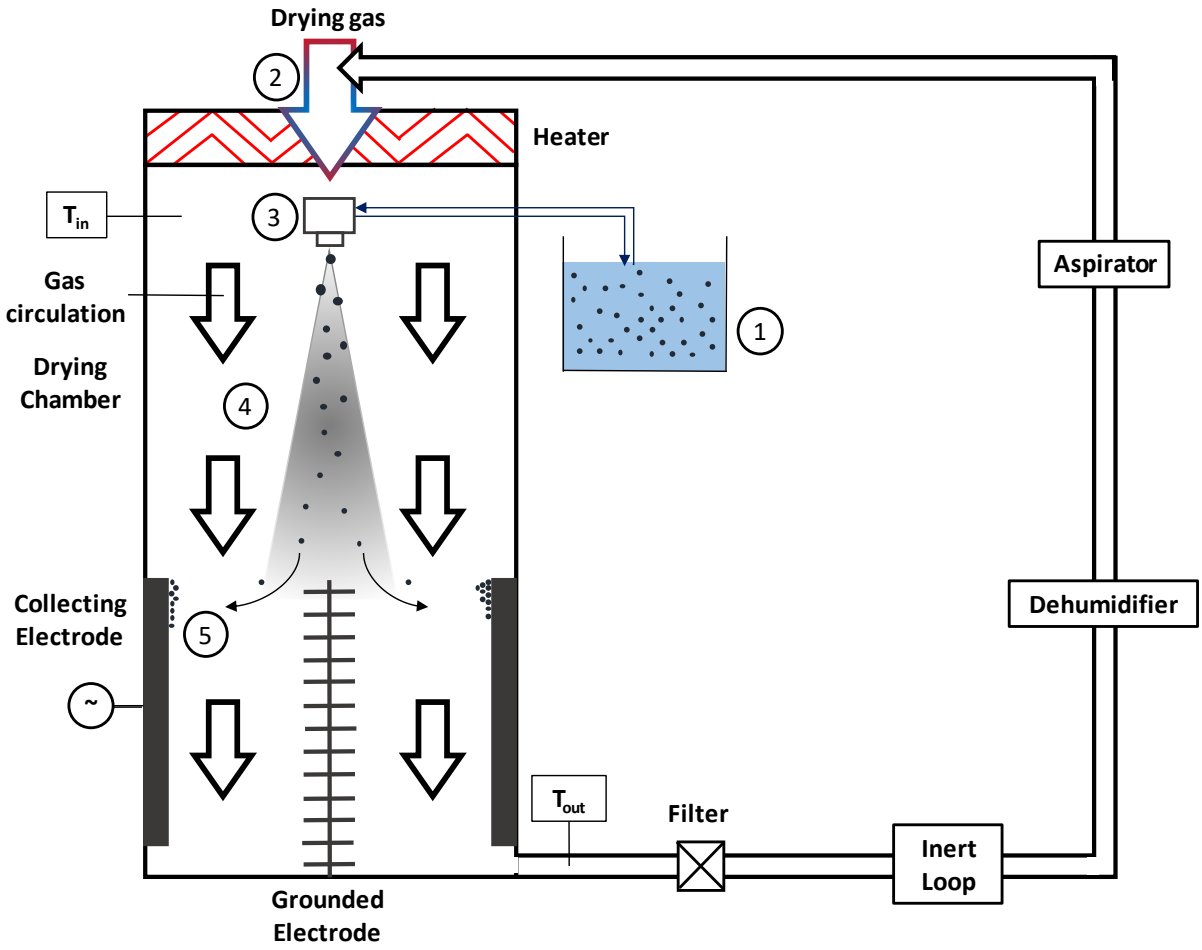

Figure 1: Flowsheet of the nano spray-drying process (adapted from [31]).

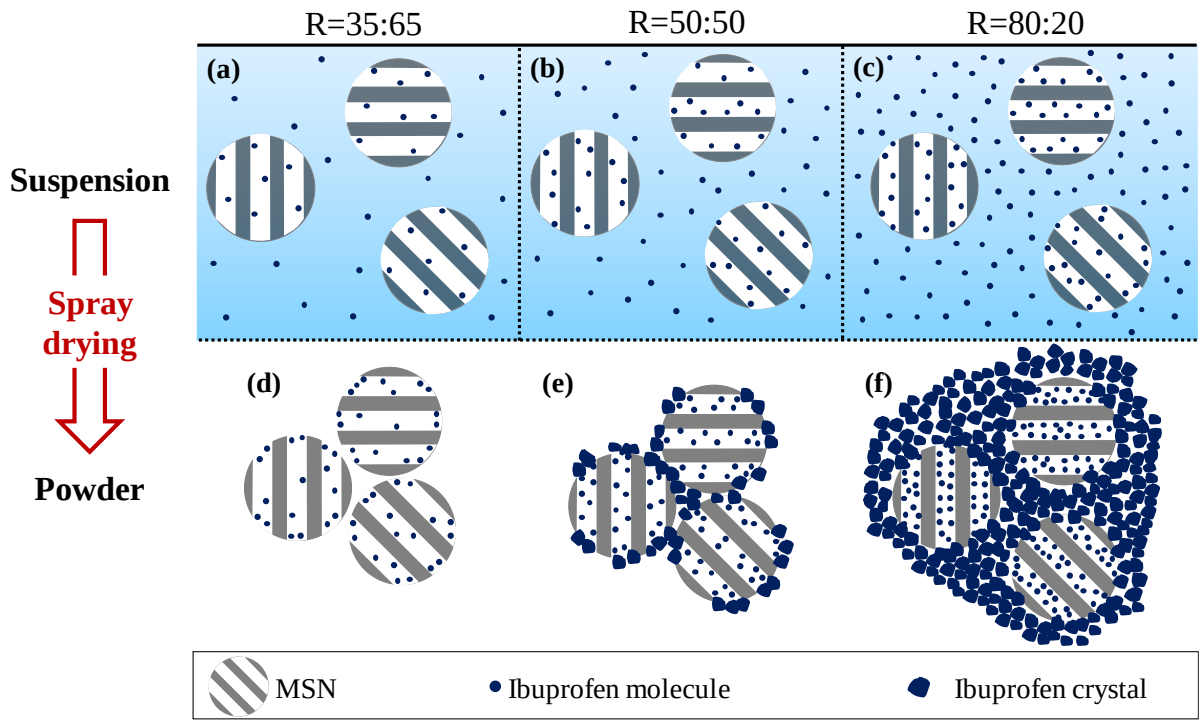

Figure 2: Schematic representation of initial suspensions with an increase of ibuprofen quantity (a, b, c) and resulting powders obtained after spray-drying (d, e, f) respectively.

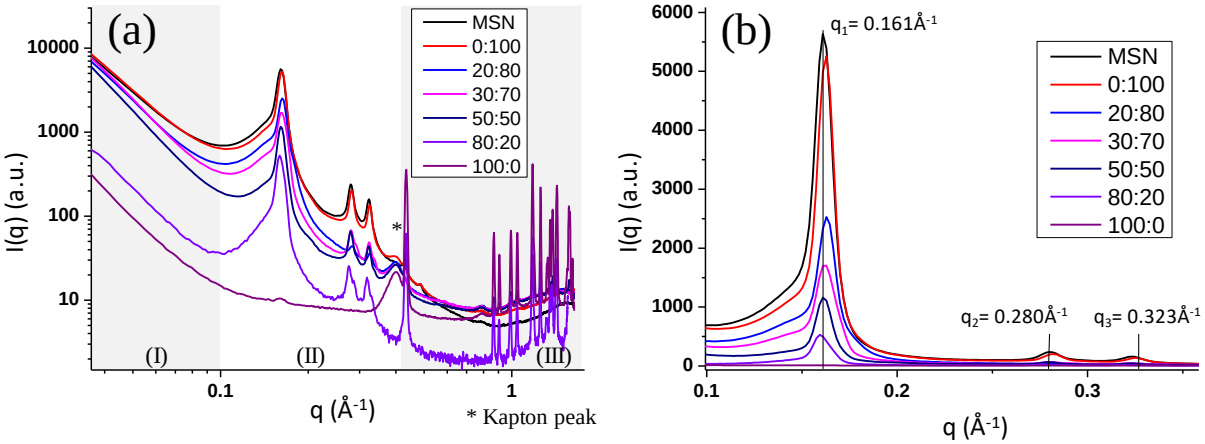

Figure 3: (a) SAXS profiles of MSN and loaded MSN at different ibuprofen/silica ratios (log/log), (b) focus on the region related to diffraction peaks of mesoporous network.

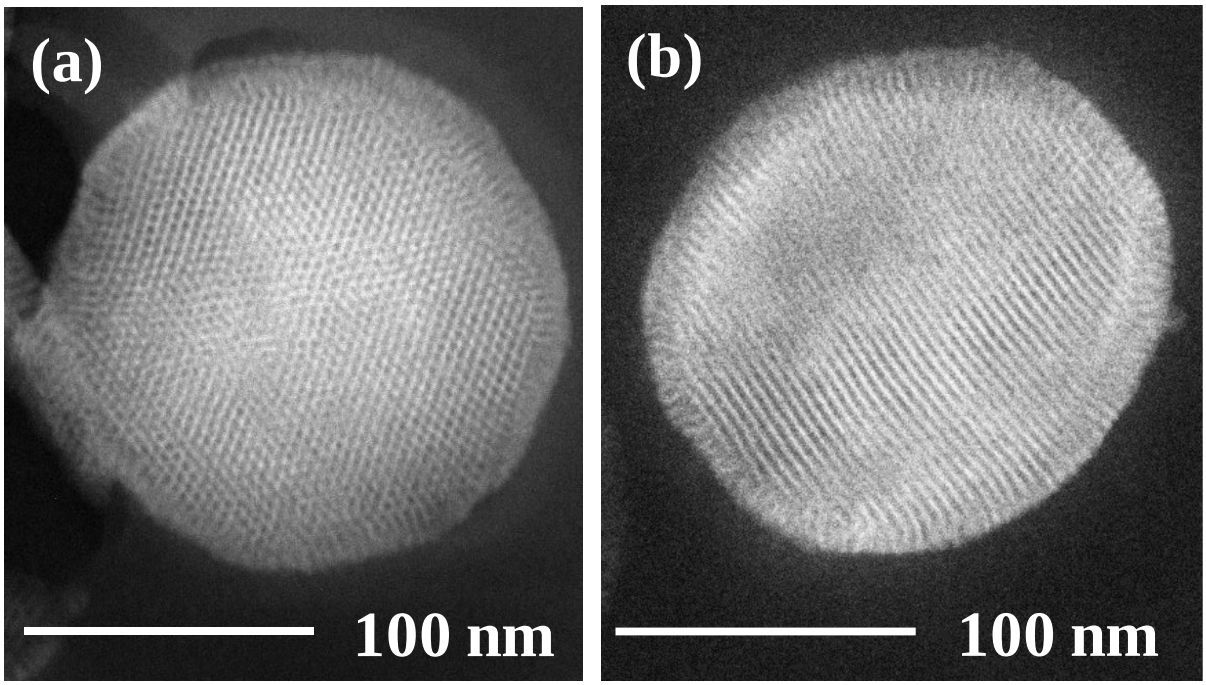

Figure 4: STEM of spray-dried MSN (R=0:100) in the axis of the pores (a) and perpendicular to the pores (b).

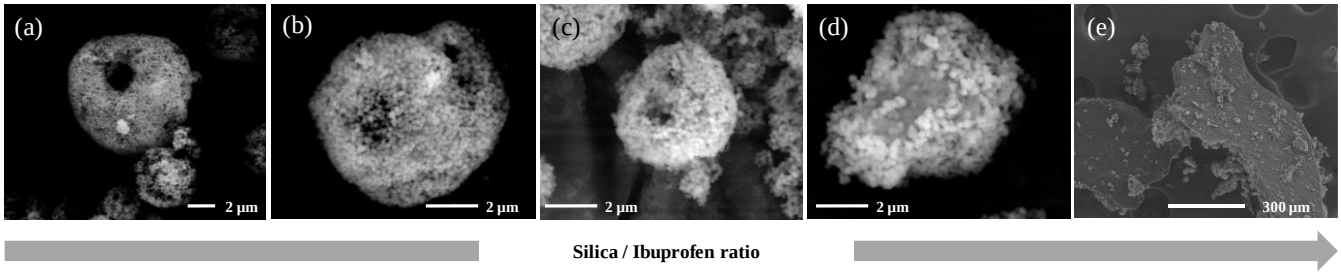

Figure 5: SEM pictures of spray-dried samples with different ibuprofen/silica ratios R : (a) 0:100, (b) 25:75, (c) 50:50, (d) 80:20, (e) 100:0.

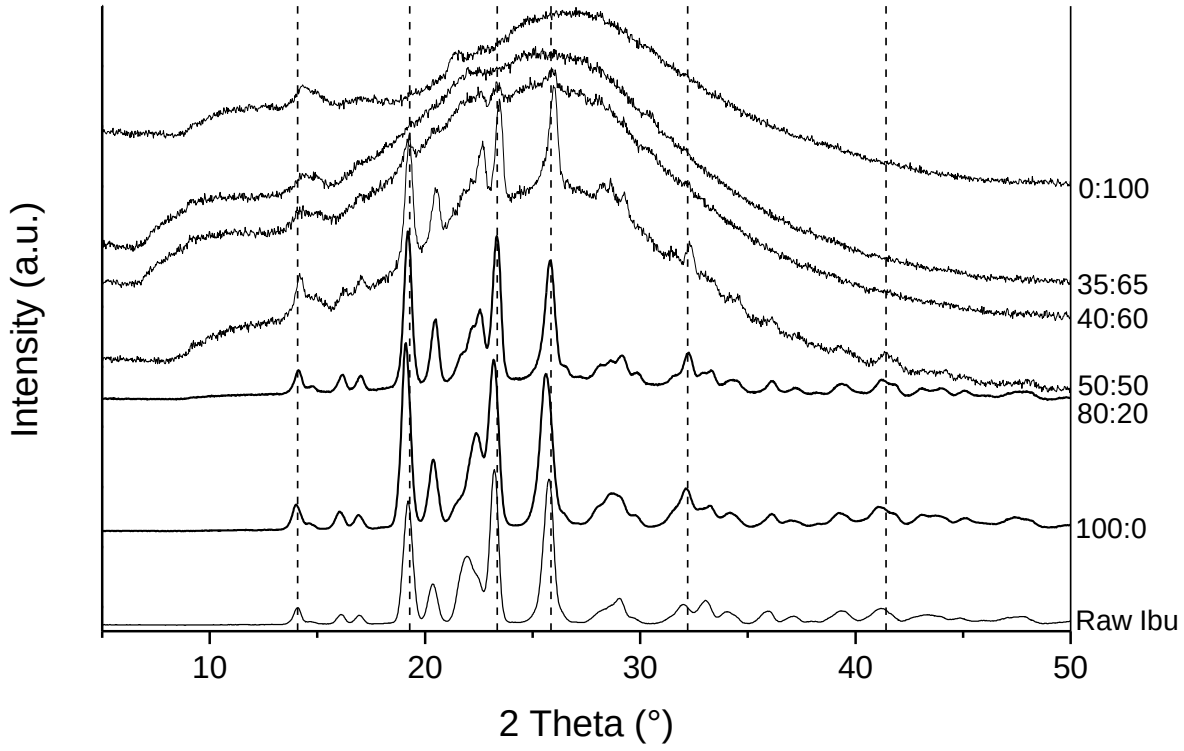

Figure 6: X-Ray diffraction patterns of raw ibuprofen and spray-dried samples with different ibuprofen/silica ratios.

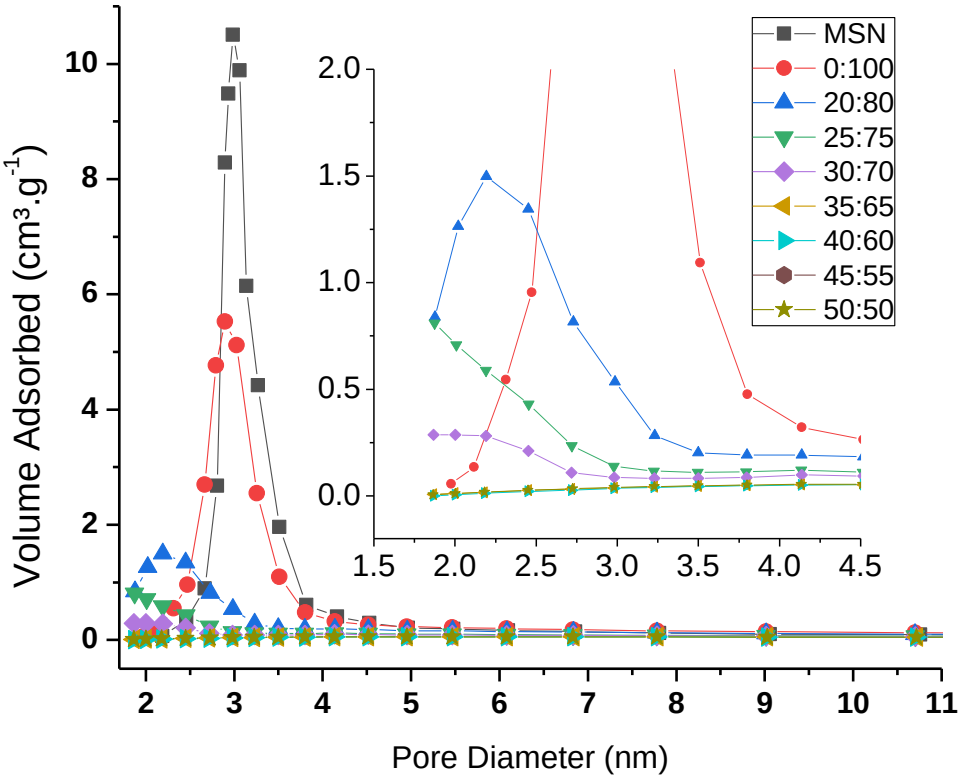

Figure 7: Pore size distributions obtained by nitrogen adsorption of MSN and spray-dried samples at different ibuprofen/silica ratios. Insert : Focus on small pore diameters.

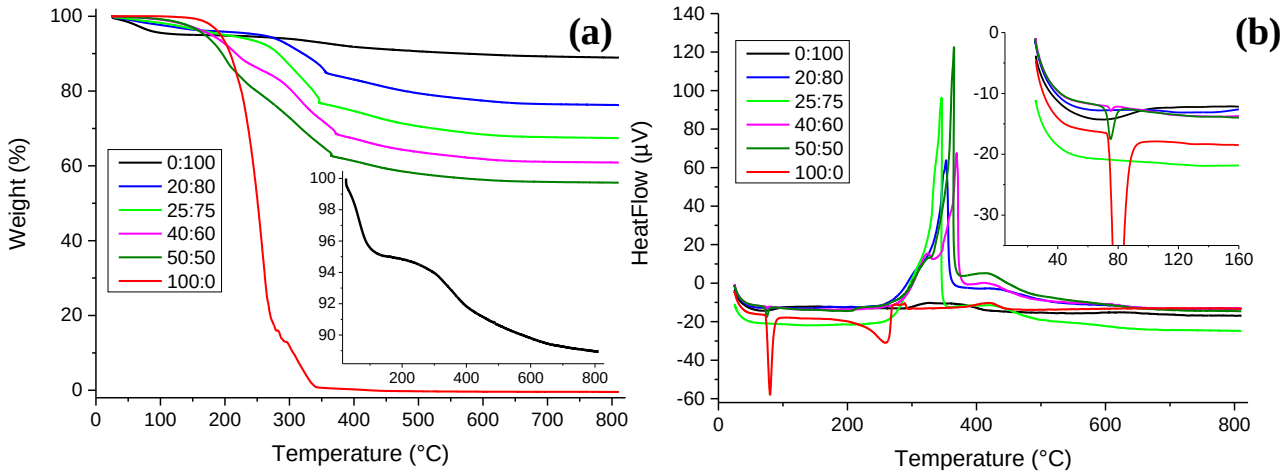

Figure 8: (a) Thermogravimetric analysis and (b) Differential thermal analysis of spray-dried samples with different ibuprofen/silica ratios. Insert on (a): Focus on the 0:100 curve, insert on (b) : Focus between 20 and 160°C.

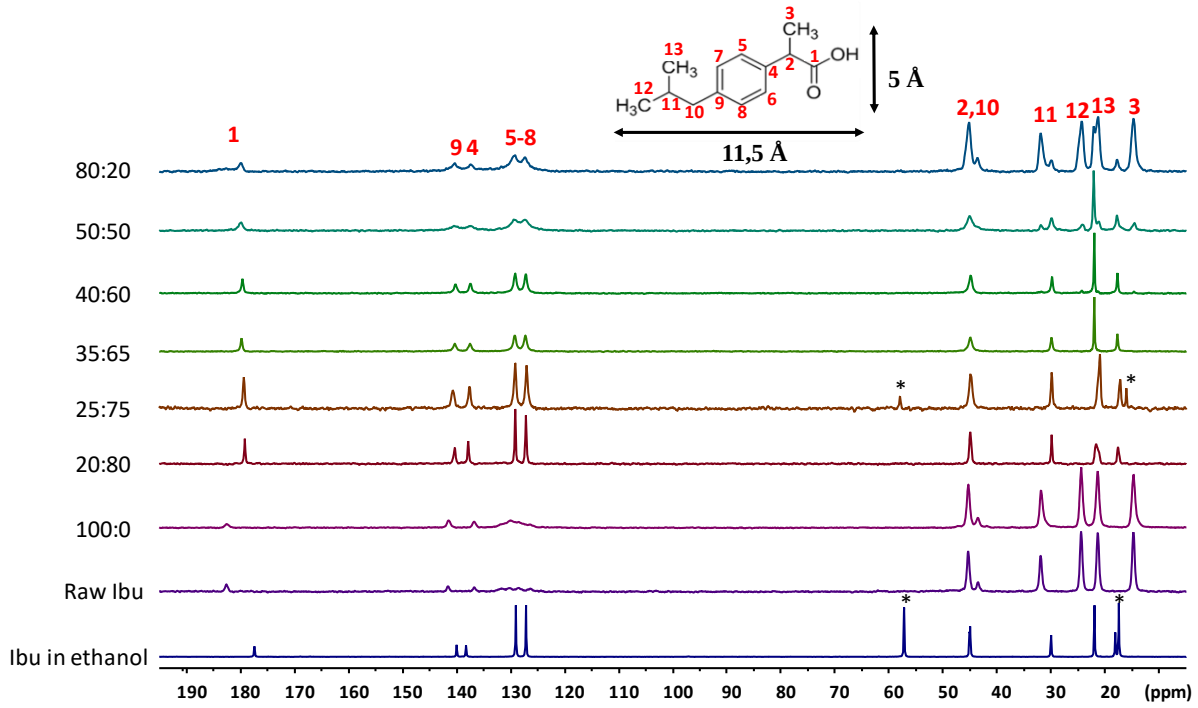

Figure 9: ^{13}C MAS spectra (relaxation delay of 5 s) of ibuprofen dissolved in ethanol, raw ibuprofen and spray-dried samples with different ibuprofen/silica ratios; *: Ethanol.

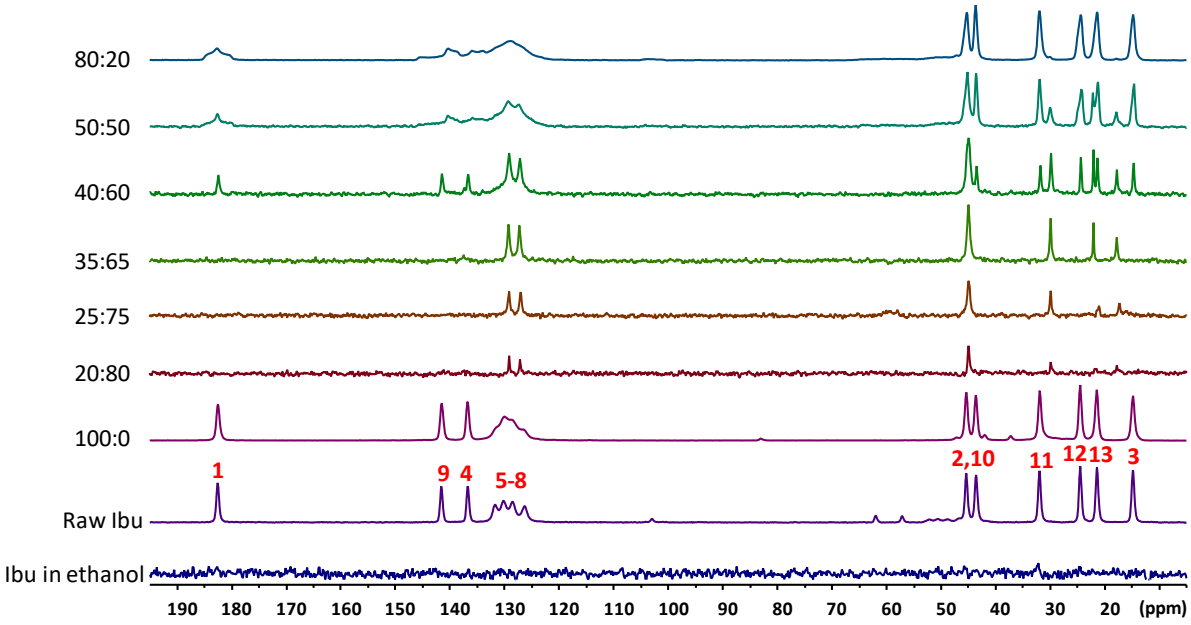

Figure 10: ^{13}C CP MAS spectra (contact time of 2 ms) of ibuprofen dissolved in ethanol, raw ibuprofen and spray-dried samples with different ibuprofen/silica ratios.

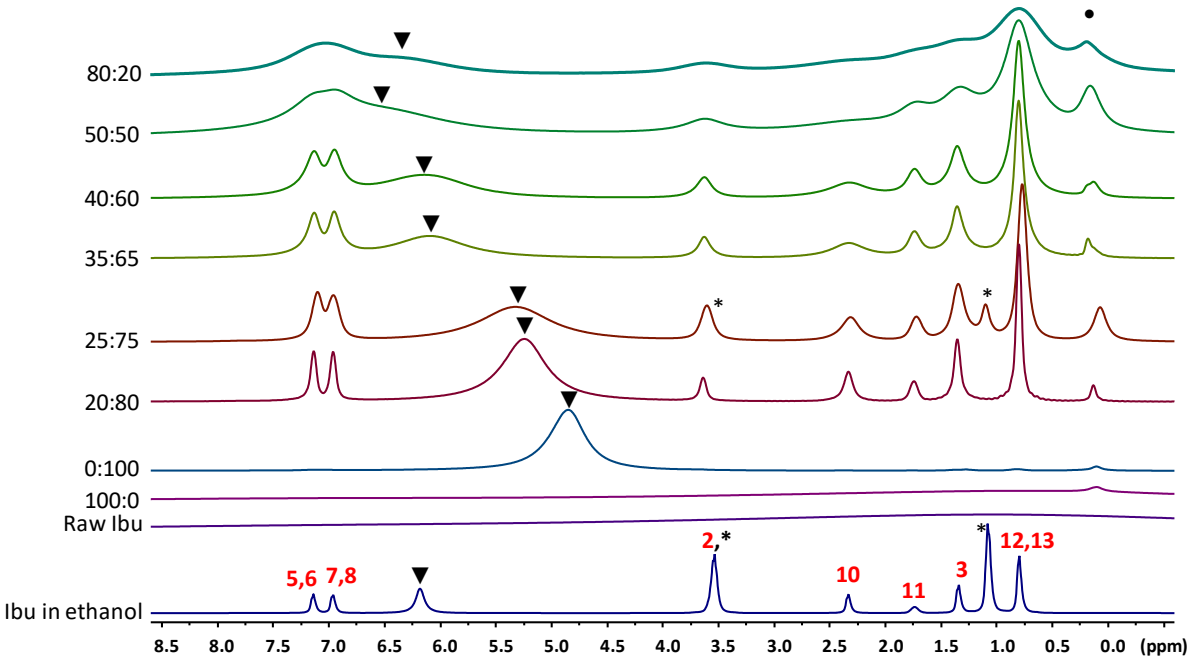

Figure 11: ^{1}H MAS spectra of ibuprofen dissolved in ethanol, raw ibuprofen and spray-dried samples with different ibuprofen/silica ratios; ▼ OH signal; *: Ethanol.

APPENDIX A : SUPPLEMENTARY DATA

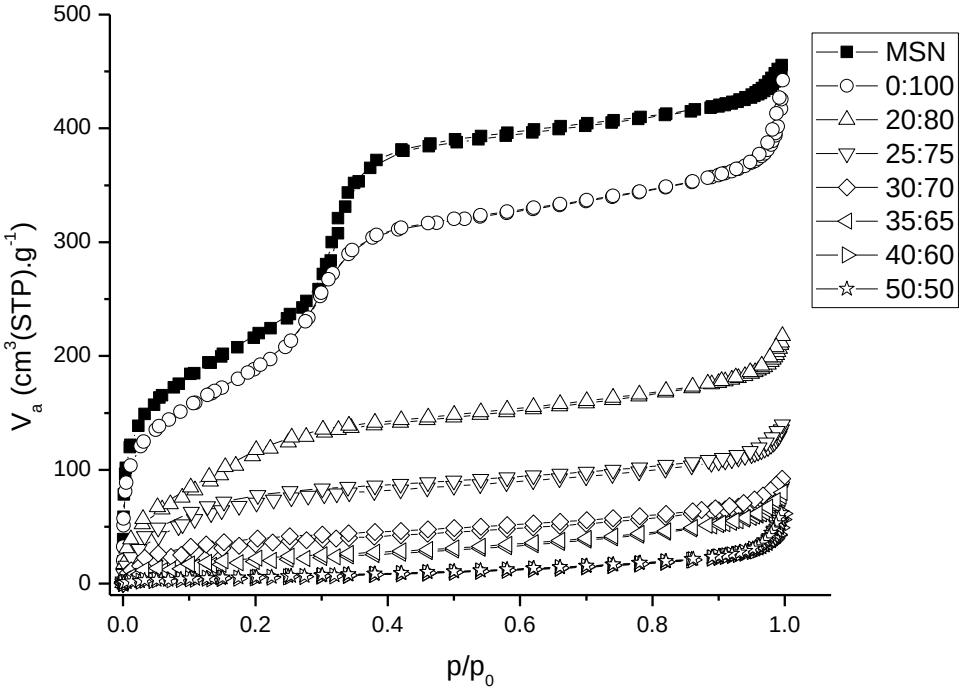

S1: Nitrogen adsorption/desorption isotherms of MSN and spray-dried samples at different ibuprofen/silica ratios

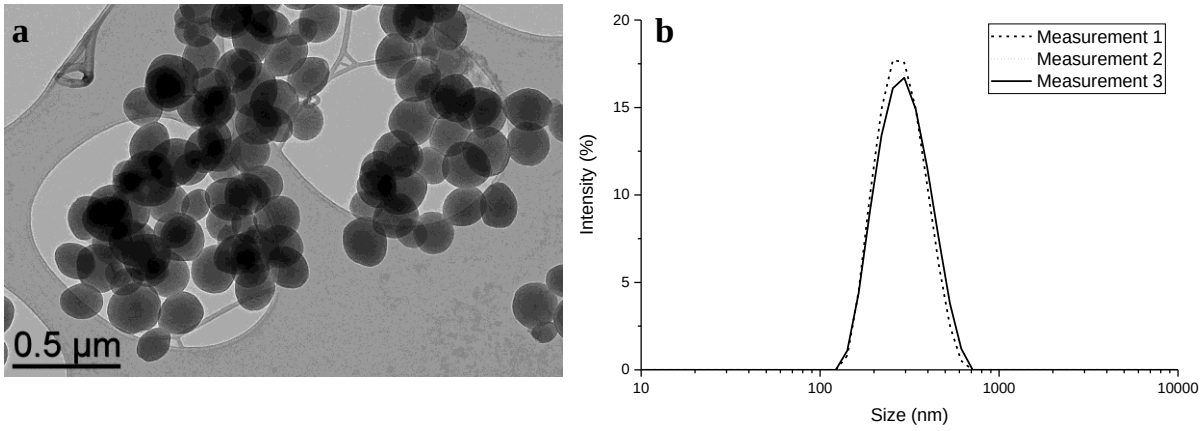

S2: a-TEM picture of MSN at low magnification and b- DLS measurements of one sample of MSN

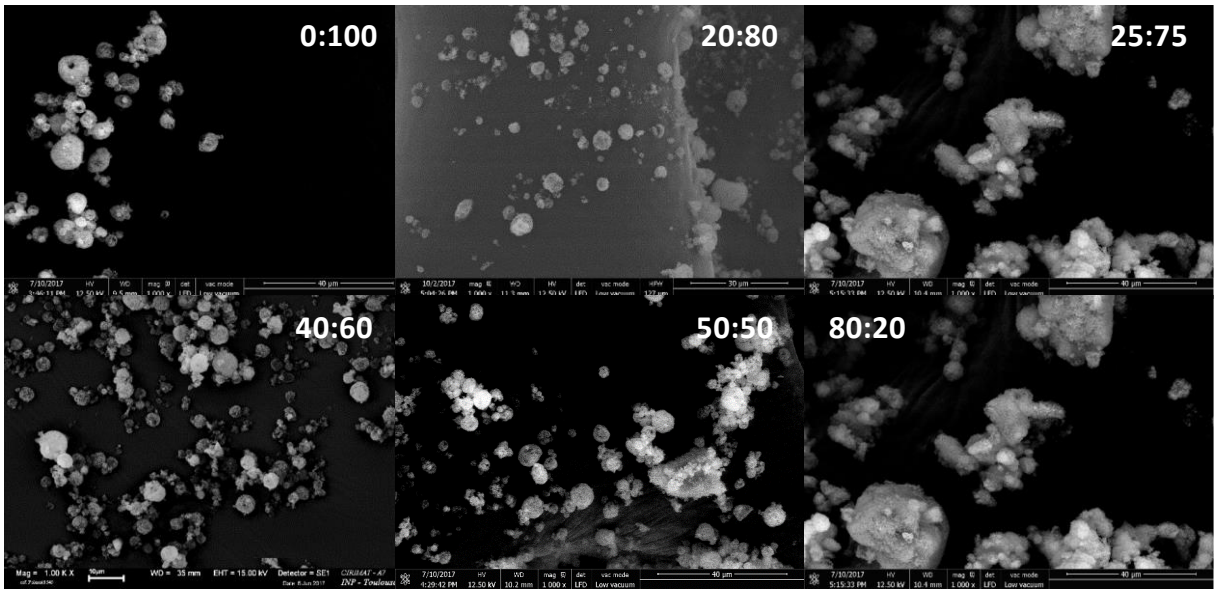

S3: SEM pictures at low magnification of spray-dried samples at different ibuprofen/silica ratios

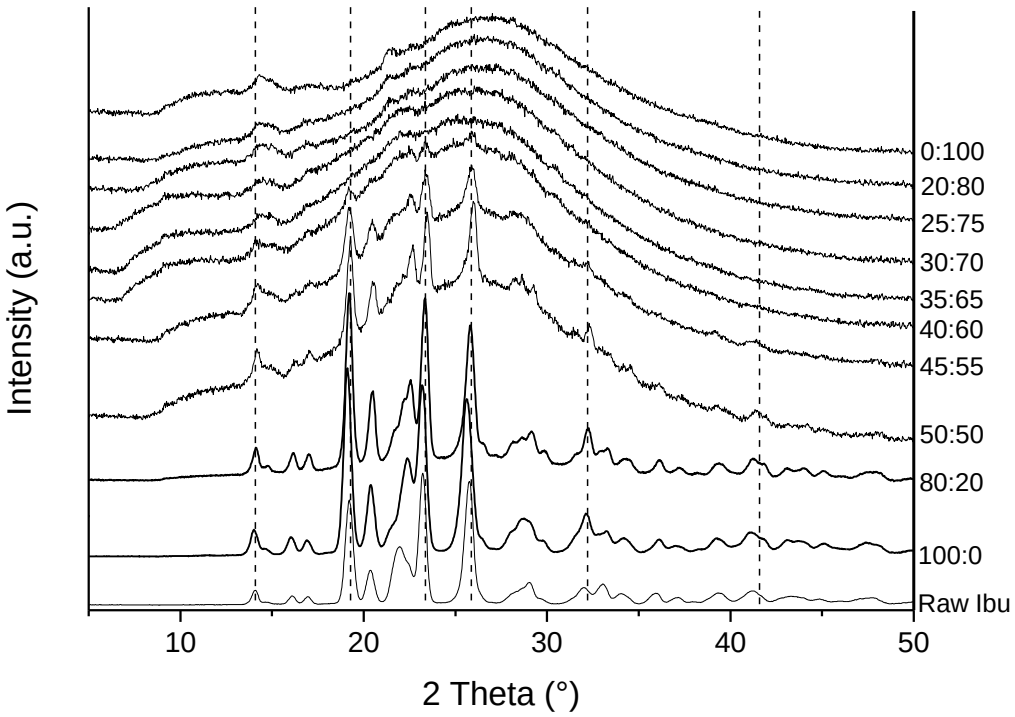

S4: X-Ray diffraction patterns of raw ibuprofen and spray-dried samples at different ibuprofen/silica ratios.

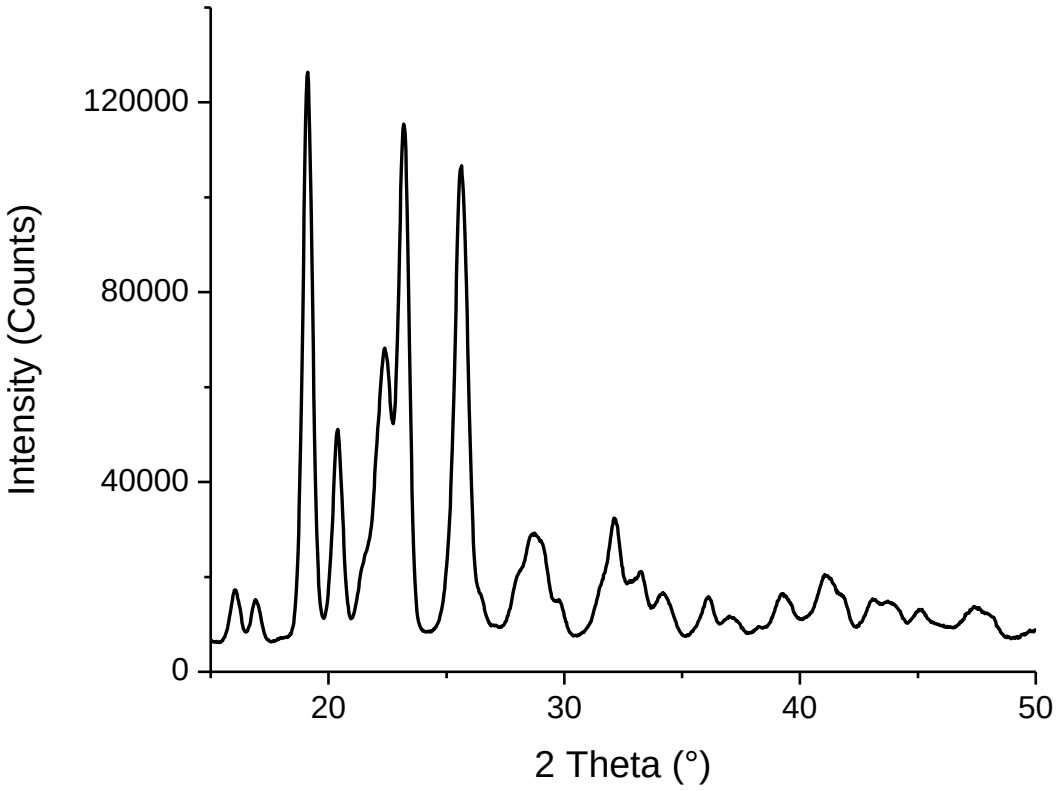

S5: X-Ray diffraction patterns of spray-dried ibuprofen (100:0)

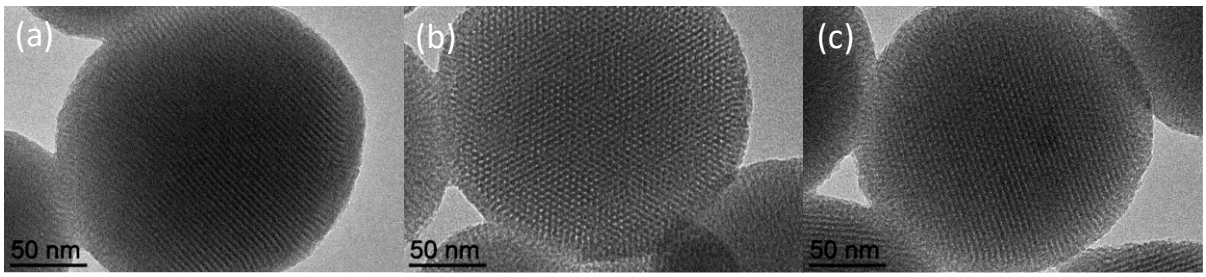

S6: TEM pictures (JEOL-1400) of spray-dried particles obtained at different ibuprofen/silica ratios (a) 25:75, (b) 30:70 and (c) 40:60.

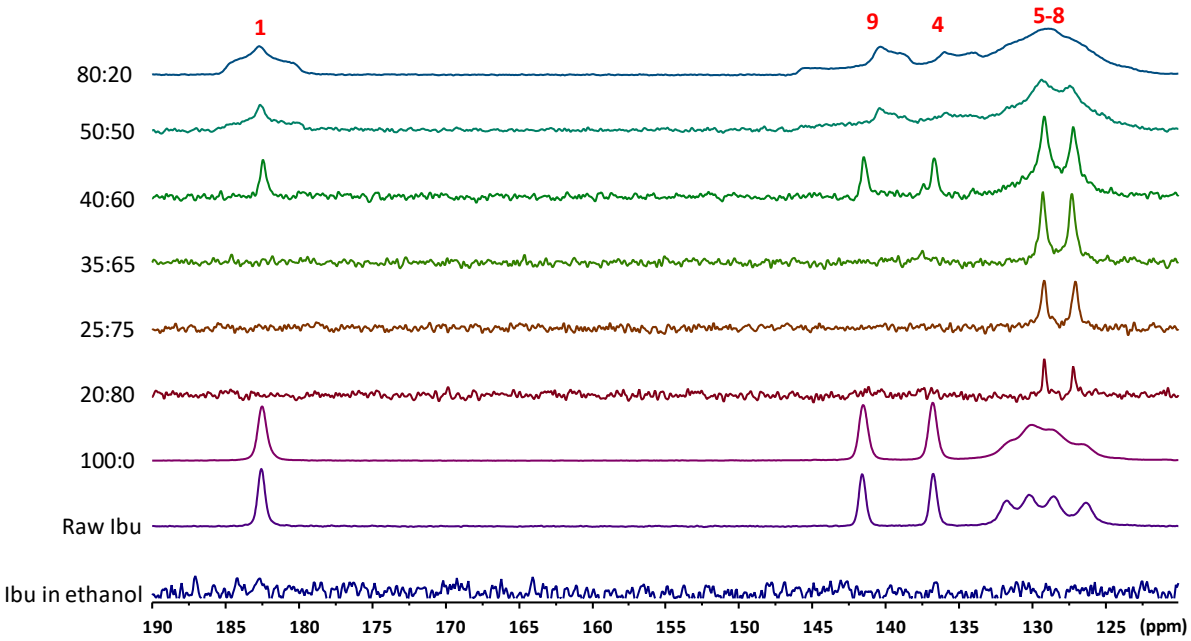

S7: Zoom of the 120-190 ppm area of the ^{13}C CP MAS spectra.

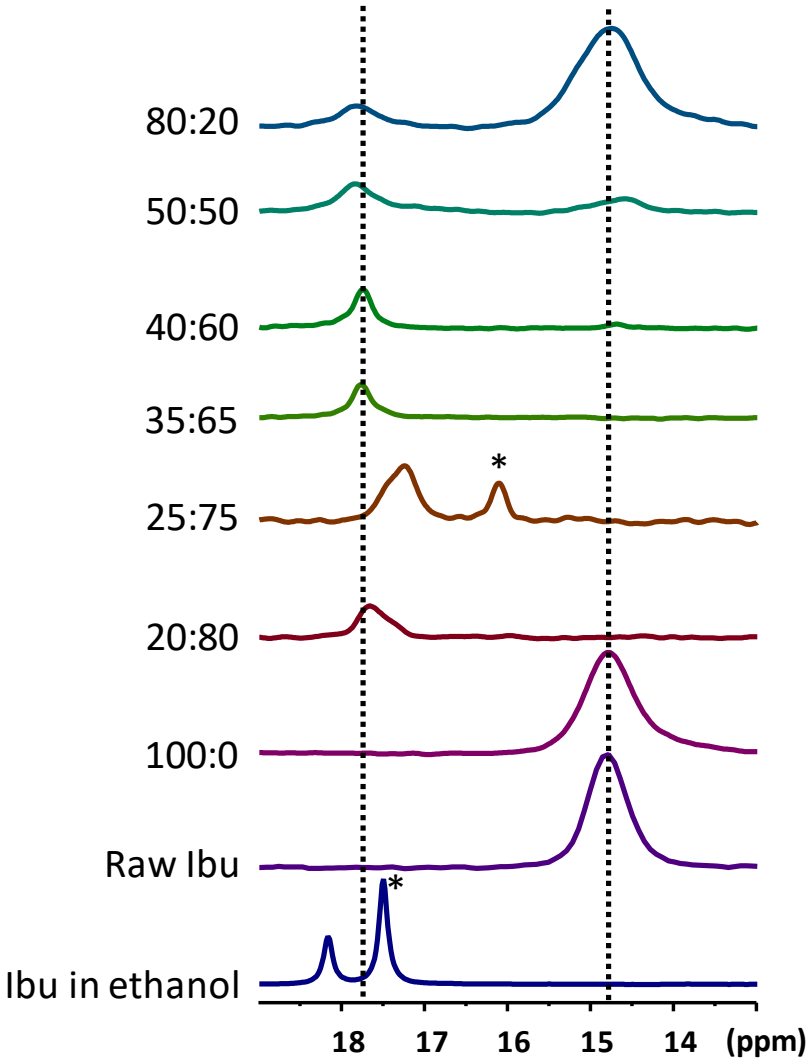

S8: Zoom of the Methyl 3 area of the ^{13}C MAS spectra.

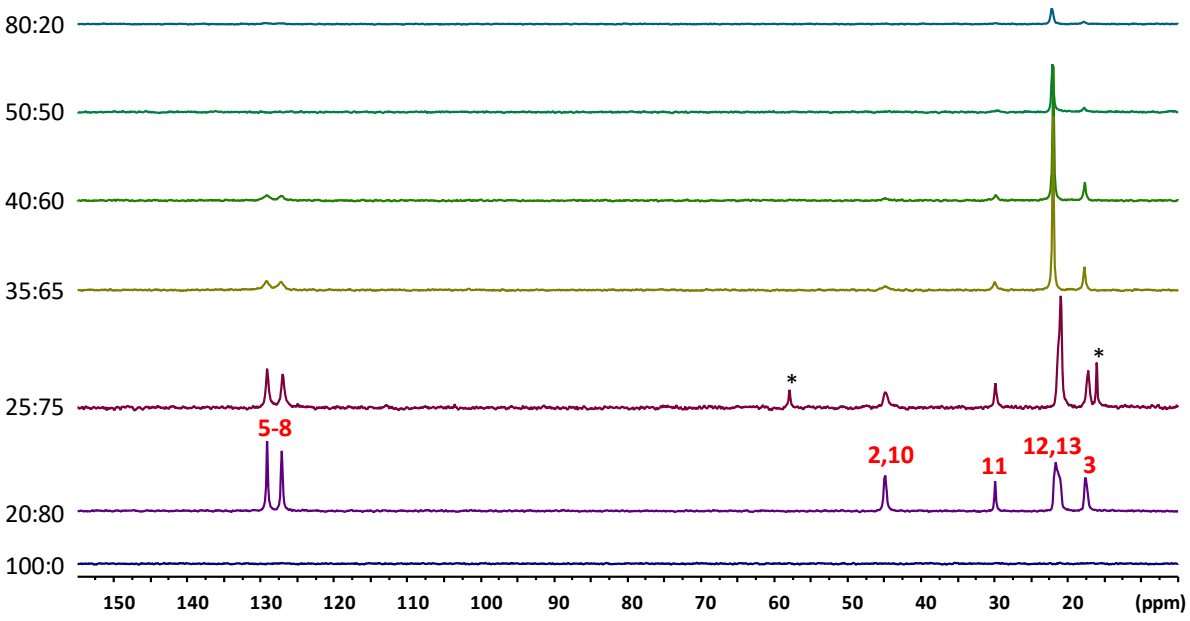

S9: ^{13}C INEPT MAS spectra (relaxation delay of 5 s); *: Ethanol.

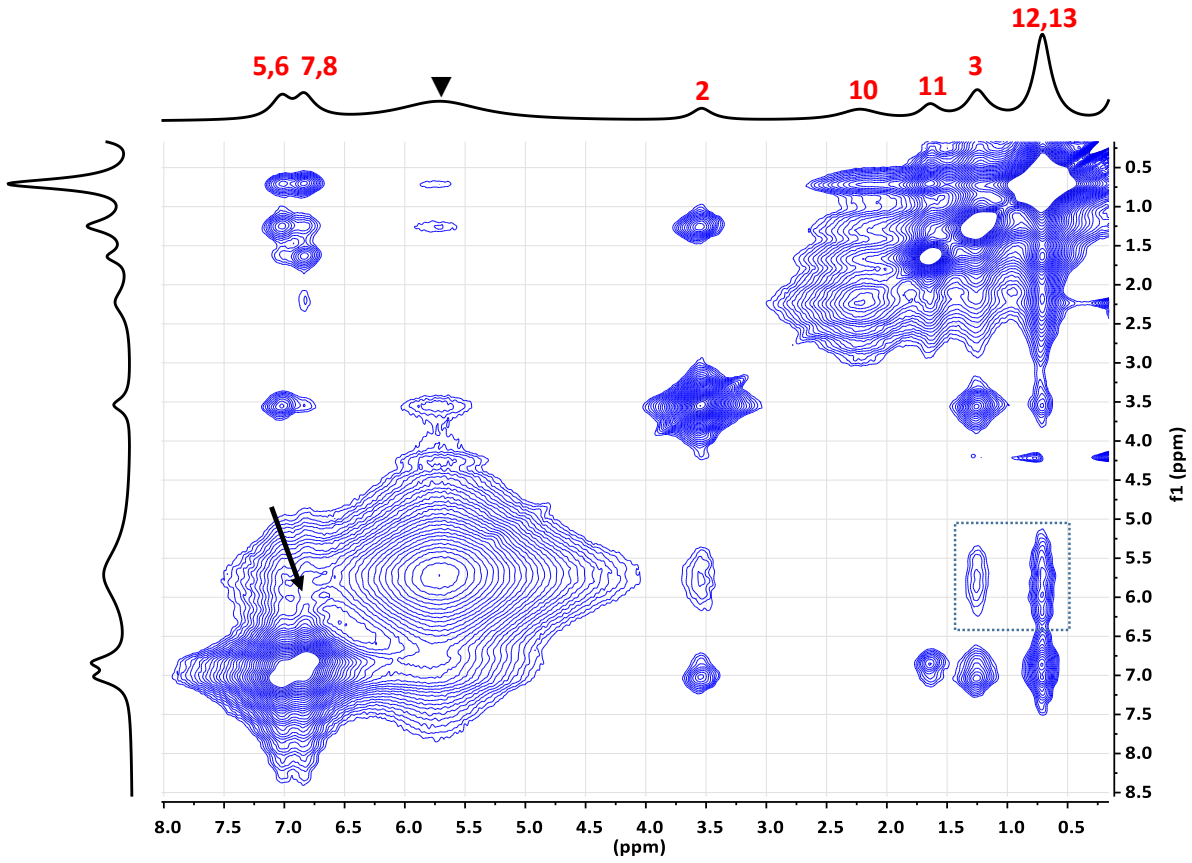

S10: ^{1}H- ^{1}H 2D NOESY experiment (mixing time of 4 ms) for R=35:65. Box: NOE cross-peaks between OH groups and Ibuprofen methyls 3 and 12,13. Arrow: NOE cross-peak between OH groups and Ibuprofen aromatic hydrogens

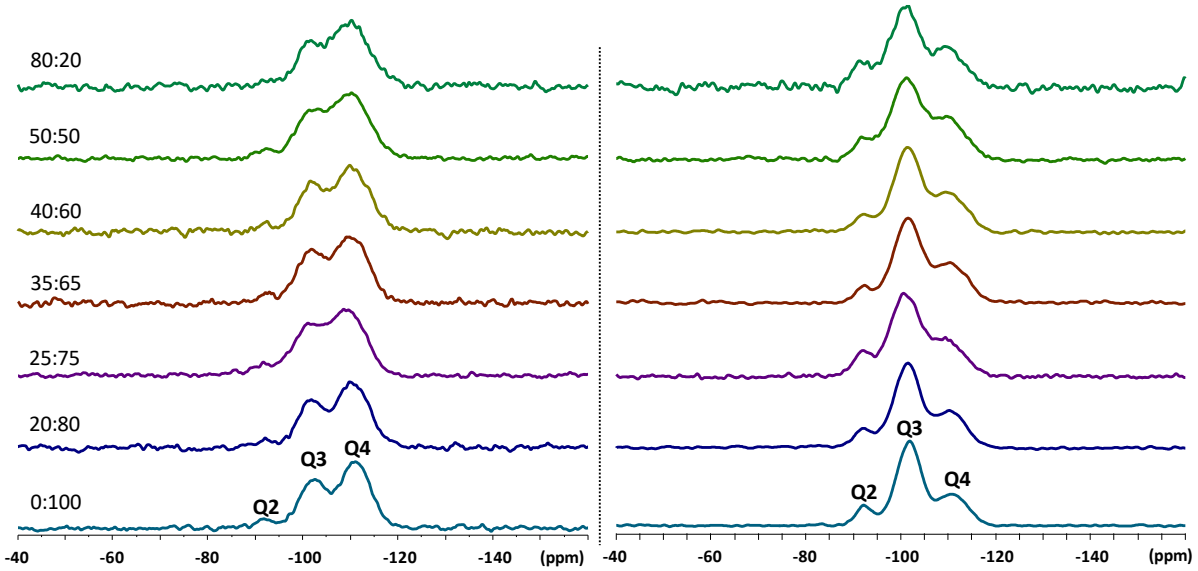

S11: ^{29}Si MAS spectra (relaxation delay of 60 s, left) and ^{29}Si CP MAS spectra (contact time of 3 ms, right).

REFERENCES

[1] T. Lian, J.Y.H Rodney, Trends and Developments in Liposome Drug Delivery Systems. J. Pharm. Sci. 90 (2001) 667–680, https://doi.org/10.1002/jps.1023

[2] Z. Li, J.C. Barnes, A. Bosoy, J.F. Stoddart, J. Zink, Mesoporous Silica Nanoparticles in Biomedical Applications. Chem. Soc. Rev, 41 (2012) 2590-2596, https://doi.org/10.1039/c1cs15246g.

[3] Y. Wang, Q. Zhao, N. Han, L.Bai, J.Li, J.Liu, E.Che, L. Hu, Q. Zhang, T. Jiang, S. Wang, Mesoporous Silica Nanoparticles in Drug Delivery and Biomedical Applications. Nanomedicine Nanotechnol. Biol. Med, 11 (2015) 313–327, https://doi.org/10.1016/j.nano.2014.09.014.

[4] J.L. Paris, M.V. Cabañas, M. Manzano, M. Vallet-Regí, Polymer-Grafted Mesoporous Silica Nanoparticles as Ultrasound-Responsive Drug Carriers. ACS Nano, 11 (2015), 11023-11033, https://doi.org/10.1021/acsnano.5b04378.

[5] M. Vallet-Regí, M. Colilla, I. Izquierdo-Barba, M. Manzano, Mesoporous Silica Nanoparticles for Drug Delivery: Current Insights. Molecules, 23 (2017) 47-53, https://doi.org/10.3390/molecules23010047.

[6] I.I, Slowing, J.L. Vivero-Escoto, C.W. Wu, V.S.Y. Lin, Mesoporous Silica Nanoparticles as Controlled Release Drug Delivery and Gene Transfection Carriers. Adv. Drug Deliv. Rev. 60 (2008), 1278-1288, https://doi.org/10.1016/j.addr.2008.03.012.

[7] Y. Zhang, Z. Zhi, T. Jiang, J. Zhang, Z. Wang, S. Wang, Spherical Mesoporous Silica Nanoparticles for Loading and Release of the Poorly Water-Soluble Drug Telmisartan. J. Controlled Release, 145 (2010) 257–263, https://doi.org/10.1016/j.jconrel.2010.04.029.

[8] L. Jia, J. Shen, Z. Li, D. Zhang, Q. Zhang, C. Duan, G. Liu, D. Zheng, Y. Liu, X. Tian, Successfully Tailoring the Pore Size of Mesoporous Silica Nanoparticles: Exploitation of Delivery Systems for Poorly Water-Soluble Drugs, Int. J. Pharm., 439 (2012), 81–91, https://doi.org/10.1016/j.ijpharm.2012.10.011.

[9] I.I. Slowing, J.L. Vivero-Escoto, B.G. Trewyn, V.S.Y. Lin, Mesoporous Silica Nanoparticles: Structural Design and Applications. J. Mater. Chem., 37 (2010) 7924-7932, https://doi.org/10.1039/c0jm00554a.

[10] W. Gao, J.M. Chan, O. Farokhzad, PH-Responsive Nanoparticles for Drug Delivery. Mol. Pharm. 7 (2010) 1913–1920, https://doi.org/10.1021/mp100253e.

[11] R.R. Castillo, M. Vallet-Regí, Functional Mesoporous Silica Nanocomposites: Biomedical Applications and Biosafety, Int. J. Mol. Sci., 20 (2019) 929-936, https://doi.org/10.3390/ijms20040929.

[12] W.D. Bossaert, D.E. De Vos, W.M. Van Rhijn, J. Bullen, P.J. Grobet, P.A. Jacobs, Mesoporous Sulfonic Acids as Selective Heterogeneous Catalysts for the Synthesis of Monoglycerides, J. Catal., 182 (1999) 156–164, https://doi.org/10.1006/jcat.1998.2353

[13] M. Vallet-Regí, Ordered Mesoporous Materials in the Context of Drug Delivery Systems and Bone Tissue Engineering, Chem. Eur. J., 12 (2006) 5934–5943, https://doi.org/10.1002/chem.200600226.

[14] V. Mamaeva, J.M. Rosenholm, L.T. Bate-Eya, L. Bergman, E. Peuhu, A. Duchanoy, L.E. Fortelius, S. Landor, D. Toivola, L. Lindén, C. Sahlgren, Mesoporous Silica Nanoparticles as Drug Delivery Systems for Targeted Inhibition of Notch Signaling in Cancer, Mol. Ther., 19 (2011) 1538–1546, https://doi.org/10.1038/mt.2011.105.

[15] T. Heikkilä, J. Salonen, J. Tuura, N. Kumar, T. Salmi, D.Y. Murzin, M.S. Hamdy, G. Mul, L. Laitinen, A.M. Kaukonen, J. Hirvonen, V.P Lehto, Evaluation of Mesoporous TCPSi, MCM-41, SBA-15, and TUD-1 Materials as API Carriers for Oral Drug Delivery, Drug Deliv. 14 (2007) 337–347, https://doi.org/10.1080/10717540601098823.

[16] M. Vallet-Regi, A. Rámila, R.P. del Real, J.A. Pérez-Pariente, New Property of MCM-41: Drug Delivery System, Chem. Mater., 13 (2001) 308–311, https://doi.org/10.1021/cm0011559.

[17] T. Numpilai, S. Muenmee, T. Witoon, Impact of Pore Characteristics of Silica Materials on Loading Capacity and Release Behavior of Ibuprofen, Mater. Sci. Eng. C, 59 (2016) 43–52, https://doi.org/10.1016/j.msec.2015.09.095.

[18] R. Mellaerts, J.A. Jammaer, M. Van Speybroeck, H. Chen, J. Van Humbeeck, P. Augustijns, G. Van den Mooter, J.A. Martens, Physical State of Poorly Water Soluble Therapeutic Molecules Loaded into SBA-15 Ordered Mesoporous Silica Carriers: A Case Study with Itraconazole and Ibuprofen, Langmuir 24 (2008) 24 8651–8659, https://doi.org/10.1021/la801161g.

[19] S. Shen, W.K. Ng, L. Chia, Y. Dong, R.B.H. Tan, Stabilized Amorphous State of Ibuprofen by Co-Spray Drying With Mesoporous SBA-15 to Enhance Dissolution Properties, J. Pharm. Sci., 99 (2010) 1997–2007, https://doi.org/10.1002/jps.21967.

[20] I. Izquierdo-Barba, E. Sousa, J.C. Doadrio, A.L. Doadrio, J.P. Pariente, A. Martínez, F. Babonneau, M. Vallet-Regí, Influence of Mesoporous Structure Type on the Controlled Delivery of Drugs: Release of Ibuprofen from MCM-48, SBA-15 and Functionalized SBA-15, J. Sol-Gel Sci. Technol., 50 (2009), 421–429, https://doi.org/10.1007/s10971-009-1932-3.

[21] F. Babonneau, L. Yeung, N. Steunou, C. Gervais, A. Ramila, M. Vallet-Regi, Solid State NMR Characterisation of Encapsulated Molecules in Mesoporous Silica, J. Sol-Gel Sci. Technol., 31 (2004), 219–223, https://doi.org/10.1023/B:JSST.0000047991.73840.8b

[22] T. Azaïs, C. Tourné-Péteilh, F. Aussenac, N. Baccile, C. Coelho, J.M. Devoisselle, F. Babonneau, Solid-State NMR Study of Ibuprofen Confined in MCM-41 Material, Chem. Mater., 18 (2006) 6382–6390, https://doi.org/10.1021/cm061551c

[23] X. Du, J. He, Regulation role of ibuprofen toward the morphology of porous silica nanospheres during its in situ encapsulation, J. Coll. Int. Sci, 345 (2010), 269-277. https://doi.org/10.1016/j.jcis.2010.02.012

[24] Brás, A. R.; Merino, E. G.; Neves, P. D.; Fonseca, I. M.; Dionísio, M.; Schönhals, A.; Correia, N. T. Amorphous Ibuprofen Confined in Nanostructured Silica Materials: A Dynamical Approach. *J. Phys. Chem. C*, *115* (2011), 4616–4623. https://doi.org/10.1021/jp107631m

[25] S.C. Shen, W.K. Ng, L. Chia, J. Hu, R.B.H. Tan, Physical State and Dissolution of Ibuprofen Formulated by Co-Spray Drying with Mesoporous Silica: Effect of Pore and Particle Size, Int. J. Pharm., 410 (2011), 188–195. https://doi.org/10.1016/j.ijpharm.2011.03.018.

[26] X. Li, X. Du, J. He, Self-Cleaning Antireflective Coatings Assembled from Peculiar Mesoporous Silica Nanoparticles, Langmuir, 26 (2010) 135258-13534 https://doi.org/10.1021/la1016824

[27] M. Vogt, K. Kunath, J.B. Dressman, Dissolution Enhancement of Fenofibrate by Micronization, Cogrinding and Spray-Drying: Comparison with Commercial Preparations, Eur. J. Pharm. Biopharm., 68 (2008) 283–288, https://doi.org/10.1016/j.ejpb.2007.05.010.

[28] M. Fatnassi, C. Tourné-Péteilh, T. Mineva, J.M. Devoisselle, P. Gaveau, F. Fayon, B. Alonso, Drug Nano-Domains in Spray-Dried Ibuprofen–Silica Microspheres, Phys. Chem. Chem. Phys., 14 (2012) 12285-12296, https://doi.org/10.1039/c2cp42092a.

[29] X. Li, N. Anton, C. Arpagaus, F. Belleteix, T. Vandamme, Nanoparticles by Spray Drying Using Innovative New Technology: The Büchi Nano Spray Dryer B-90, J. Controlled Release, 147 (2010) 304–310, https://doi.org/10.1016/j.jconrel.2010.07.113.

[30] K. Bürki, I. Jeon, C. Arpagaus, G. Betz, New Insights into Respirable Protein Powder Preparation Using a Nano Spray Dryer, Int. J. Pharm., 408 (2011) 248–256, https://doi.org/10.1016/j.ijpharm.2011.02.012.

[31] C. Arpagaus, Novel Laboratory-Scale Spray Dryer to Produce Nanoparticles. Dry. Technol., 30 (2012) 1113–1121, https://doi.org/10.1080/07373937.2012.686949.

[32] K. Schmid, C. rpagaus, W. Friess, Evaluation of the Nano Spray Dryer B-90 for Pharmaceutical Applications, Pharm. Dev. Technol., 16 (2011) 287–294, https://doi.org/10.3109/10837450.2010.485320.

[33] B. Muñoz, A. Rámila, J. Pérez-Pariente, I. Díaz, M. Vallet-Regí, MCM-41 Organic Modification as Drug Delivery Rate Regulator, Chem. Mater., 15 (2003), 500–503, https://doi.org/10.1021/cm021217q.

[34] S.W. Song, K. Hidajat, S. Kawi, Functionalized SBA-15 Materials as Carriers for Controlled Drug Delivery: Influence of Surface Properties on Matrix–Drug Interactions, Langmuir 21 (2005), 9568–9575, https://doi.org/10.1021/la051167e.

[35] C. Tourné-Péteilh, D. Brunel, S. Bégu, B. Chiche, F. Fajula, D.A. Lerner, J.M. Devoisselle, Synthesis and Characterisation of Ibuprofen-Anchored MCM-41 Silica and Silica Gel, New J. Chem., 27 (2003), 1415–1418, https://doi.org/ 10.1039/B307046H

[36] P. Yang, Z. Quan, L. Lu, S. Huang, J. Lin, H. Fu, MCM-41 Functionalized with YVO_4:Eu^{3+}: A Novel Drug Delivery System, Nanotechnology, 18 (2007) 235703-235708, https://doi.org/10.1088/0957-4484/18/23/235703.

[37] I.I. Slowing, B.G. Trewyn, V.S.Y. Lin, Effect of Surface Functionalization of MCM-41-Type Mesoporous Silica Nanoparticles on the Endocytosis by Human Cancer Cells, J. Am. Chem. Soc., 46 (2006) 14792–14793, https://doi.org/10.1021/ja0645943.

[38] R. Narayan, U. Nayak, A. Raichur, S. Garg, Mesoporous Silica Nanoparticles: A Comprehensive Review on Synthesis and Recent Advances. Pharmaceutics, 10 (2018), 118-125, https://doi.org/10.3390/pharmaceutics10030118.

[39] C. Arpagaus, Nano Spray Dryer B-90: Literature Review and Applications, Dry. Technol. 30 (2011) 1113–1121.

[40] R.C Murdock, L. Braydich-Stolle, A.M. Schrand, J.J. Schlager, S. Hussain, Characterization of Nanomaterial Dispersion in Solution Prior to In Vitro Exposure Using Dynamic Light Scattering Technique, Toxicol. Sci., 101 (2008) 239–253, https://doi.org/10.1093/toxsci/kfm240.

[41] E.P. Barrett, L.G. Joyner, P.P. Halenda, The Determination of Pore Volume and Area Distributions in Porous Substances. I. Computations from Nitrogen Isotherms, J. Am. Chem. Soc., 73 (1951) 373–380.

[42] S. Brunauer, P.H. Emmett, E. Teller, Adsorption of Gases in Multimolecular Layers, J. Am. Chem. Soc., 60 (1938) 309–319.

[43] K.S.W. Sing, D.H. Everett, R.A.W. Haul, L. Moscou, R.A. Pierotti, J. Rouquerol, Siemieniewska, Reporting Physisorption Data for Gas/Solid Systems, Pure Appl. Chem., 57 (1985) 603-619.

[44] A. Abd-Elbary, M.A. El Nabarawi, D.H. Hassen, A.A. Taha, Inclusion and Characterization of Ketoprofen into Different Mesoporous Silica Nanoparticles Using Three Loading Methods, Int. J. Pharm. Pharm. Sci., 6 (2014) 183–191.

[45] K. Möller, J. Kobler, T. Bein, Colloidal Suspensions of Nanometer-Sized Mesoporous Silica. Adv. Funct. Mater., 17 (2007) 605–612, https://doi.org/10.1002/adfm.200600578.

[46] A.B.D. Nandiyanto, K. Okuyama, Progress in Developing Spray-Drying Methods for the Production of Controlled Morphology Particles: From the Nanometer to Submicrometer Size Ranges, Adv. Powder Technol, 22 (2011) 1–19, https://doi.org/10.1016/j.apt.2010.09.011.

[47] Y. Wang, K. Kho, W.S. Cheow, K.A. Hadinoto, Comparison between Spray Drying and Spray Freeze Drying for Dry Powder Inhaler Formulation of Drug-Loaded Lipid–Polymer Hybrid Nanoparticles, Int. J. Pharm., 424 (2012) 98–106, https://doi.org/10.1016/j.ijpharm.2011.12.045.

[48] M. Faustini, M. Giraud, D. Jones, J. Rozière, M. Dupont, T.R. Porter, S. Nowak, M. Bahri, O. Ersen, O.; C. Sanchez, C. Boissiere, C. Tard, J. Peron, Hierarchically Structured Ultraporous Iridium-Based Materials: A Novel Catalyst Architecture for Proton Exchange Membrane Water Electrolyzers, Adv. Energy Mater., 9 (2019) 1802136-1802147, https://doi.org/10.1002/aenm.201802136.

[49] R. Pérez-Masiá, R. López-Nicolás, M.J Periago, G. Ros, J.M. Lagaron, A. López-Rubio, Encapsulation of Folic Acid in Food Hydrocolloids through Nanospray Drying and Electrospraying for Nutraceutical Applications, Food Chem., 168 (2015) 124–133, https://doi.org/10.1016/j.foodchem.2014.07.051.

[50] M. Sliwinska-Bartkowiak, G. Dudziak, R. Gras, R. Sikorski, R. Radhakrishnan, K. Gubbins, Freezing Behavior in Porous Glasses and MCM-41, Colloids Surf. Physicochem. Eng. Asp., 187 (2001) 523–529.

[51] S. Ramukutty, E. Ramachandran, Growth, Spectral and Thermal Studies of Ibuprofen Crystals, Cryst. Res. Technol., 47 (2012) 31–38, https://doi.org/10.1002/crat.201100394.

[52] J. Trébosc, J.W. Wiench, S. Huh, V.S.Y. Lin, M. Pruski, Solid-State NMR Study of MCM-41-Type Mesoporous Silica Nanoparticles, J. Am. Chem. Soc., 127 (2005) 3057–3068.

[53] C. Charnay, S. Bégu, C. Tourné-Péteilh, L. Nicole, D.A. Lerner, J.M. Devoisselle, Inclusion of Ibuprofen in Mesoporous Templated Silica: Drug Loading and Release Property, Eur. J. Pharm. Biopharm., 57 (2004) 533–540, https://doi.org/10.1021/ja043567e.

[54] L. Gao, J. Sun, L. Zhang, J. Wang, B. Ren, Influence of Different Structured Channels of Mesoporous Silicate on the Controlled Ibuprofen Delivery, Mater. Chem. Phys., 135 (2012) 786–797, https://doi.org/10.1016/j.matchemphys.2012.05.059.

[55] J.G. Li, G. Fornasieri, A. Bleuzen, M. Gich, A. Gloter, F. Bouquet, M. Impéror-Clerc, Alignment under Magnetic Field of Mixed Fe_2O_3 /SiO_2 Colloidal Mesoporous Particles Induced by Shape Anisotropy, Small, 12 (2016) 5981–5988, https://doi.org/10.1002/smll.201602272.

[56] C.J. Gommes, G. Prieto, P.E. De Jongh, Small-Angle Scattering Analysis of Empty or Loaded Hierarchical Porous Materials, J. Phys. Chem. C 120 (2016) 1488–1506, https://doi.org/10.1021/acs.jpcc.5b09556.

[57] J. Andersson, J. Rosenholm, S. Areva, M. Lindén, Influences of Material Characteristics on Ibuprofen Drug Loading and Release Profiles from Ordered Micro- and Mesoporous Silica Matrices. Chem. Mater., 16 (2004), 4160–4167, https://doi.org/10.1021/cm0401490.

[58] F. Wan, A. Bohr, M.J. Maltesen, S. Bjerregaard, C. Foged, J. Rantanen, M. Yang, Critical Solvent Properties Affecting the Particle Formation Process and Characteristics of Celecoxib-Loaded PLGA Microparticles via Spray-Drying, Pharm. Res., 30 (2013), 1065–1076, https://doi.org/10.1007/s11095-012-0943-x.

[59] F. Guenneau, K. Panesar, A. Nossov, A.; M.A. Springuel-Huet, T. Azaïs, F. Babonneau, C. Tourné-Péteilh, J.M. Devoisselle, A. Gédéon, Probing the Mobility of Ibuprofen Confined in MCM-41 Materials Using MAS-PFG NMR and Hyperpolarised-129Xe NMR Spectroscopy, Phys. Chem. Chem. Phys. 15 (2013) 18805-18811, https://doi.org/10.1039/c3cp52695j.